The Interaction of Dirac Particles with Non-Abelian Gauge Fields and Gravity – Bound States

Felix Finster, Joel Smoller,[*] and Shing-Tung Yau[†]

January 2000

Abstract

We consider a spherically symmetric, static system of a Dirac particle interacting with classical gravity and an $SU(2)$ Yang-Mills field. The corresponding Einstein-Dirac-Yang/Mills equations are derived. Using numerical methods, we find different types of soliton-like solutions of these equations and discuss their properties. Some of these solutions are stable even for arbitrarily weak gravitational coupling.

1 Introduction

The coupling of gravity to other classical force fields and to quantum mechanical particles has led to many interesting solutions of Einstein's equations and has given some insight into the nature of the nonlinear interactions. The first such examples are the Bartnik-McKinnon (BM) solutions of the Einstein-Yang/Mills (EYM) equations [1]. For these solutions, the repulsive Yang-Mills force compensates the attractive gravitational force; unfortunately, these solutions are unstable [2]. If, on the other hand, one considers quantum mechanical Dirac particles, the gravitational attraction is balanced by the repulsion due to the Heisenberg Uncertainty Principle, and this leads to stable bound states of the resulting Einstein-Dirac (ED) system [3]. However, a pure ED system is somewhat artificial, because physical Dirac particles also exhibit electroweak and strong interactions, which in all realistic situations are much stronger than gravity. Thus the question arises if Dirac particles in a gravitational field still form bound states if an additional strong coupling to a non-abelian Yang-Mills (YM) field is taken into account (the case of an abelian gauge field was considered in [4]). Related questions are, do the BM solutions become stable if one includes Dirac particles, and which physical effects does the nonlinear coupling in the Einstein-Dirac-Yang/Mills (EDYM) equations lead to?

In order to address these questions, we consider here a static, spherically symmetric EDYM system of one Dirac particle in a gravitational field and an $SU(2)$ Yang-Mills field. In this system, the spinors couple only to the magnetic component of the YM field, and we thus obtain a consistent ansatz by setting the electric component identically equal to zero. In the limit of weak coupling of the spinors, our system goes over to the EYM system [1]. In contrast to the two-particle singlet state studied in [3], we consider here only one Dirac particle (this becomes possible because the inclusion of the $SU(2)$ Yang-Mills field changes the representation of the rotation group on the spinors; see Section 2). Thus one cannot

---

recover exactly the ED system [3], but the limit of a weak Yang-Mills field yields equations which are closely related to the ED equations of the two-particle singlet.

By numerically seeking bound states of the EDYM system, we find a surprisingly rich solution structure. First of all, we find solutions where the Dirac particle is bound by the gravitational attraction, and where the Dirac particle also generates a YM field. Stable solutions of this type exist also in the physically realistic situation of weak gravitational and strong YM coupling. This result shows that the magnetic component of the YM field, which usually has a repulsive effect (like e.g. for the BM solutions) cannot prevent Dirac particles from forming stable bound states. We also find other types of solutions where the binding comes about through the nonlinear interaction of all three fields. These solutions have stable and unstable branches, whereby the stable solutions are found for weak gravitational coupling, provided that the YM coupling is sufficiently strong, but not too strong. Finally, we study the relation between these solutions and the BM solutions. We find one-parameter families of solutions which join the BM ground state with our new solutions. This shows that the BM ground state can be made stable by the inclusion of a Dirac particle, but only if the coupling to the spinors is sufficiently strong. The first excited BM state, on the other hand, cannot be joined with our new solutions. Namely, perturbing this state by an additional Dirac particle yields a separate unstable branch of EDYM solutions.

The plan of the paper is as follows. In Section 2 we derive the $SU(2)$-EDYM equations. In Section 3 we obtain a limiting system constructed by letting the gravitational constant tend to zero and letting the YM coupling constant tend to infinity. We find numerical solutions of this system and discuss their properties. In the last section, we consider solutions of the full EDYM equations, obtained by tracing the solutions of our limiting system and the BM solutions while continuously varying the coupling constants.

2   Derivation of the Equations

The general EDYM equations are obtained by variation over Lorentzian metrics g_{ij}, YM connections $\mathcal{A}$, and Dirac wave functions Ψ, of the action

$$S \; = \; \int \left(\frac{1}{16\pi\,\kappa}\,R \, + \, \overline{\Psi}(G-m)\Psi \, - \, \frac{1}{16\pi\,e^2}\,\mathrm{Tr}(F_{ij}\,F^{ij}) \right) \sqrt{-\det g}\, d^4x \quad , \qquad (2.1)$$

where R is scalar curvature, G is the Dirac operator (which depends on the gravitational and YM fields), F_{ij} is the YM field tensor, and where the trace is taken over the YM index. The gravitational and YM coupling constants are denoted by κ and e, respectively. The appearance of the factor e^{-2} in (2.1) requires a brief explanation. In contrast to the usual form of the gauge-covariant derivative $D_j = \partial_j - ieA_j$, we use here the convention $D_j = \partial_j - iA_j$ (this makes it possible to work with the particularly convenient form of the gauge potentials used in [1]). Our convention is obtained from the usual one by the transformation $A_j \to e^{-1} A_j$. Under this transformation, the field strength tensor behaves like $F_{ij} \to e^{-1} F_{ij}$, and this gives rise to the factor e^{-2} in (2.1).

In this paper, we shall study a particular EDYM system, which is obtained as follows. First of all, we consider a spherically symmetric, static metric in polar coordinates,

$$ds^2 \; = \; \frac{1}{T(r)^2}\,dt^2 \, - \, \frac{1}{A(r)}\,dr^2 \, - \, r^2\,d\vartheta^2 \, - \, r^2\,\sin^2\vartheta\,d\varphi^2 \quad , \qquad (2.2)$$

2

with positive functions A and T. The Einstein tensor corresponding to this metric is given in [3]. Moreover, as in [1], we restrict attention to the magnetic component of an $SU(2)$ Yang-Mills field and choose for the YM potential the ansatz

$$\mathcal{A} = w(r)\,\tau^1\,d\vartheta + (\cos\vartheta\,\tau^3 + w(r)\,\sin\vartheta\,\tau^2)\,d\varphi \tag{2.3}$$

with a real function w, where $\vec{\tau} = \frac{1}{2}\,\vec{\sigma}$ is the standard basis of $su(2)$ ($\vec{\sigma}$ are the Pauli matrices). The YM current j and energy-momentum tensor $T^i_j = \frac{1}{4\pi e^2}\,\mathrm{Tr}\,(F^{ia}F_{ja} - \frac{1}{4}\,F^{ab}F_{ab}\,\delta^i_j)$ are computed to be

$$j = \frac{1}{4\pi e^2}\left(-\frac{A}{2r^2}\,w'' - \frac{A'T - 2AT'}{4r^2\,T}\,w' - \frac{w(1-w^2)}{2r^4}\right)\left(\sigma^1\frac{\partial}{\partial\vartheta} + \sigma^2\,\csc(\vartheta)\,\frac{\partial}{\partial\varphi}\right)$$

$$T^0_0 = \frac{1}{4\pi e^2}\left(-\frac{2}{r^4}\,(1-w^2)^2 - \frac{4}{r^2}\,A\,w'^2\right) \tag{2.4}$$

$$T^1_1 = \frac{1}{4\pi e^2}\left(-\frac{2}{r^4}\,(1-w^2)^2 + \frac{4}{r^2}\,A\,w'^2\right) \tag{2.5}$$

$$T^2_2 = T^3_3 = \frac{1}{4\pi e^2}\left(\frac{2}{r^4}\,(1-w^2)^2\right)\quad, \tag{2.6}$$

and all other components vanish. When coupled to the Dirac spinors, the YM potential (2.3) has the disadvantage that it depends on ϑ and φ, in a way which makes it difficult to separate variables in the Dirac equation. To remedy this, we perform the $SU(2)$ gauge transformation $\mathcal{A}_j \to U\mathcal{A}_j U^{-1} + iU(\partial_j U^{-1})$ with

$$U(\vartheta,\varphi) = \exp\left(-i\varphi\,\tau^1\right)\exp\left(-i(\vartheta+\pi)\,\tau^3\right)\exp\left(\frac{i\pi}{2}\,\tau^2\right)\quad.$$

The resulting YM potential is

$$\mathcal{A} = (w-1)\,r\,\sin\vartheta\,(\tau^\varphi\,d\vartheta - \tau^\vartheta\,d\varphi)\quad, \tag{2.7}$$

where we use the following "polar" linear combinations of the τ matrices,

$$\tau^r = \tau^1\cos\vartheta + \tau^2\sin\vartheta\cos\varphi + \tau^3\sin\vartheta\sin\varphi$$

$$\tau^\vartheta = \frac{1}{r}\left(-\tau^1\sin\vartheta + \tau^2\cos\vartheta\cos\varphi + \tau^3\cos\vartheta\sin\varphi\right)$$

$$\tau^\varphi = \frac{1}{r\sin\vartheta}\left(-\tau^2\sin\varphi + \tau^3\cos\varphi\right)\quad. \tag{2.8}$$

By minimally coupling the $SU(2)$ potential (2.7) to the Dirac operator in the gravitational field [3, Eq. (2.23)], we obtain the Dirac operator

$$G = iT\,\gamma^t\partial_t + \gamma^r\left(i\sqrt{A}\partial_r + \frac{i}{r}\,(\sqrt{A}-1) - \frac{i}{2}\,\sqrt{A}\,\frac{T'}{T}\right) + i\gamma^\vartheta\partial_\vartheta + i\gamma^\varphi\partial_\varphi$$

$$+ \frac{2i}{r}\,(w-1)\,(\vec{\gamma}\vec{\tau} - \gamma^r\tau^r)\,\tau^r\quad, \tag{2.9}$$

where $(\gamma^j)_{j=t,r,\vartheta,\varphi}$ are, in analogy to (2.8), the Dirac matrices of Minkowski space in polar coordinates, where we work in the Dirac representation,

$$\gamma^t = \begin{pmatrix} \mathbb{1} & 0 \\ 0 & -\mathbb{1} \end{pmatrix}\quad, \qquad \vec{\gamma} = \begin{pmatrix} 0 & \vec{\sigma} \\ -\vec{\sigma} & 0 \end{pmatrix}\quad. \tag{2.10}$$

3

Notice that the Dirac operator (2.9) acts on 8-component wave functions; this is because the additional YM index doubles the number of components compared to usual Dirac spinors. More precisely, it is convenient to regard the wave functions as sections of

$$\mathbb{C}^8 \;=\; \mathbb{C}^2_{\text{up/down}} \otimes \mathbb{C}^2_{\text{large/small}} \otimes \mathbb{C}^2_{\text{YM}} \quad, \tag{2.11}$$

where $\mathbb{C}^2_{\text{up/down}}$ describes the two spin orientations, $\mathbb{C}^2_{\text{large/small}}$ corresponds to the upper and lower components of the Dirac spinor (i.e., usual Dirac spinors are sections of $\mathbb{C}^4 = \mathbb{C}^2_{\text{up/down}} \otimes \mathbb{C}^2_{\text{large/small}}$), and $\mathbb{C}^2_{\text{YM}}$ is acted upon by the $SU(2)$ gauge group. For clarity, we shall refer to the factors in (2.11) by separate indices, i.e. we write a wave function Ψ as $(\Psi^{\alpha u a})_{\alpha, u, a = 1,2}$, where α, u, and a label the components of $\mathbb{C}^2_{\text{up/down}}$, $\mathbb{C}^2_{\text{large/small}}$, and $\mathbb{C}^2_{\text{YM}}$, respectively. Thus the operators $\vec{\tau}$ act on the index a, the spin operators $\vec{S}$ are given by $\vec{S} = \frac{1}{2}\vec{\sigma}$ acting on the Greek indices, and γ^t coincides with the matrix $\gamma^t = \text{diag}(1,-1)$ acting on the index u, i.e.

$$\gamma^t\, \Psi^{\alpha u a} \;=\; \begin{cases} \Psi^{\alpha u a} & \text{if } u = 1 \\ -\Psi^{\alpha u a} & \text{if } u = 2 \end{cases} \quad.$$

It is apparent in (2.9) that the Dirac operator commutes with the three operators

$$\vec{J} \;=\; \vec{L} + \vec{S} + \vec{\tau} \quad, \tag{2.12}$$

where $\vec{L}$ is angular momentum. It is very convenient to regard the operators $\vec{J}$ as the total angular momentum operators of the system. Since the total angular momentum operators are the infinitesimal generators of rotations (as explained for angular momentum in [5, par. 26]), we can then interpret (2.12) as saying that the inclusion of the YM field influences the representation of the rotation group on the spinors. The Dirac operator is invariant under this group representation, because the operators $\vec{J}$ commute with G; this makes spherical symmetry of the Dirac operator manifest.

Since (2.12) coincides with the formula for the addition of angular momentum $\vec{L}$ to two spin-$\frac{1}{2}$-operators $\vec{S}$ and $\vec{\tau}$, it is clear that the operators $\vec{J}$ have integer eigenvalues. Thus we can expect that the operator J^2 has a nontrivial kernel. In this case, the simplest spherically symmetric ansatz for the Dirac particles would be to take one Dirac particle whose wave function is in the kernel of J^2. We now work out this ansatz in detail, whereby we consider $\vec{J}$ as operators on the spinors $\Phi^{\alpha a}(\vartheta, \varphi)$ on S^2 (i.e. the $\Phi^{\alpha a}$ are sections of $\mathbb{C}^4 = \mathbb{C}^2_{\text{up/down}} \otimes \mathbb{C}^2_{\text{YM}}$). Adding the two spin operators $\vec{S}$ and $\vec{\tau}$, we can decompose $\mathbb{C}^2_{\text{up/down}} \otimes \mathbb{C}^2_{\text{YM}}$ into the direct sum of one state of total spin zero and three states of total spin one (see [5, par. 31]; these states are usually called the singlet and triplet states, respectively). By subsequently adding the angular momentum $\vec{L}$ according to the standard rules for the addition of angular momentum [5, par. 31], one sees that the operator J^2 has indeed a nontrivial kernel. More precisely, the kernel of J^2 is two-dimensional, spanned by two vectors Φ_0 and Φ_1 with angular momentum zero and one, respectively. The state Φ_0 is (up to a phase) uniquely characterized by the conditions

$$\vec{L}\, \Phi_0 \;=\; 0 \;=\; (\vec{S} + \vec{\tau})\, \Phi_0 \qquad \text{and} \qquad \|\Phi_0\|_{S^2} \;=\; 1 \quad. \tag{2.13}$$

Using (2.13), we can write Φ_1 as

$$\Phi_1 \;=\; 2S^r\, \Phi_0 \;=\; -2\tau^r\, \Phi_0 \quad. \tag{2.14}$$

Namely, representing S^r and τ^r in the form

$$S^r = \vec{x}\vec{s} \qquad \text{and} \qquad \tau^r = \vec{x}\vec{\tau} \ ,$$

and using the standard commutation relations between the components of $\vec{L}$, $\vec{x}$, and $\vec{S}$ (see [5, pars. 26 and 54]), we obtain that

$$
\begin{aligned}
\vec{J}\,\Phi_1 &= 2\,[\vec{J},\,S^r]\,\Phi_0 = 2\,[\vec{L},\,(\vec{x}\vec{S})]\,\Phi_0 + 2\,[\vec{S}+\vec{\tau},\,(\vec{x}\vec{S})]\,\Phi_0 \\
&= -2i\,\vec{x}\wedge\vec{S}\,\Phi_0 + 2i\,\vec{x}\wedge\vec{S}\,\Phi_0 = 0
\end{aligned}
\tag{2.15}
$$

(where $\wedge$ is the wedge product in IR^3), and

$$\|\Phi_1\|_{S^2}^2 = \int_{S^2} <2S^r\Phi_0,\,2S^r\Phi_0>\,d\omega = \|\Phi_0\|_{S^2}^2 = 1 \ .$$

One can verify directly that Φ_1 has angular momentum one; namely

$$
\begin{aligned}
L^2\,\Phi_1 &= 2L^2\,S^r\,\Phi_0 = 2\vec{L}\,[\vec{L},\,S^r]\,\Phi_0 = -2i\,\vec{L}(\vec{x}\wedge\vec{S})\,\Phi_0 \\
&= -2i\,[\vec{L},\,(\vec{x}\wedge\vec{S})]\,\Phi_0 = 4\,(\vec{x}\vec{S})\,\Phi_0 = l(l+1)\,\Phi_1
\end{aligned}
$$

with $l = 1$. Furthermore, using the fact that $(2S^r)^2 = 1 = (2\tau^r)^2$ and $S^2 = \frac{3}{4} = \tau^2$, we obtain that

$$\Phi_0 = 2S^r\,\Phi_1 = -2\tau^r\,\Phi_1 \tag{2.16}$$

$$\vec{S}\vec{\tau}\,\Phi_0 \overset{(2.13)}{=} -\vec{S}\vec{S}\,\Phi_0 = -\frac{3}{4}\,\Phi_0 \tag{2.17}$$

$$\vec{S}\vec{\tau}\,\Phi_1 = \frac{1}{2}\,((\vec{S}+\vec{\tau})^2 - S^2 - \tau^2)\,\Phi_1 \overset{(2.15)}{=} \frac{1}{2}\,(L^2 - S^2 - \tau^2)\,\Phi_1 = \frac{1}{4}\,\Phi_1 \tag{2.18}$$

$$\vec{S}\vec{L}\,\Phi_0 = 0 \tag{2.19}$$

$$\vec{S}\vec{L}\,\Phi_1 = \frac{1}{2}\,((\vec{S}+\vec{L})^2 - S^2 - L^2)\,\Phi_1 = \frac{1}{2}\,(\tau^2 - S^2 - L^2)\,\Phi_1 = -\Phi_1 \ . \tag{2.20}$$

Finally, it is useful to observe that (cf. [6, equation (3.3)])

$$S^\vartheta\partial_\vartheta + S^\varphi\partial_\varphi = -\frac{2}{r}\,S^r\,(\vec{S}\vec{L}) \ . \tag{2.21}$$

Using the relations (2.13)–(2.21), one can easily compute the Dirac operator (2.9) on the invariant subspace $J^2 = 0$. It turns out that we obtain a consistent ansatz for the Dirac wave function by setting

$$\Psi^{\alpha u a}(t,r,\vartheta,\varphi) = e^{-i\omega t}\,\frac{\sqrt{T(r)}}{r}\,(\alpha(r)\,\Phi_0^{\alpha a}(\vartheta,\varphi)\,\delta_{u,1} + i\beta(r)\,\Phi_1^{\alpha a}(\vartheta,\varphi)\,\delta_{u,2}) \tag{2.22}$$

with real functions α and β, where $\omega > 0$ is the energy of the Dirac particle, and $\delta_{.,.}$ is the Kronecker delta. For this ansatz, the Dirac equation reduces to the system of ODEs

$$\sqrt{A}\,\alpha' = \frac{w}{r}\,\alpha - (m + \omega T)\,\beta \tag{2.23}$$

$$\sqrt{A}\,\beta' = (-m + \omega T)\,\alpha - \frac{w}{r}\,\beta \ . \tag{2.24}$$

5

The Dirac current j and Dirac energy-momentum tensor $T_{jk} = \mathrm{Re}\,(\overline{\Psi} G_{(j} D_{k)} \Psi)$ corresponding to the ansatz (2.22) are obtained by a straightforward computation similar to that in [3]. The result is

$$
j = -\frac{2T}{r^3}\,\alpha\beta \left(\sigma^1 \frac{\partial}{\partial\vartheta} + \sigma^2 \csc(\vartheta) \frac{\partial}{\partial\varphi} \right)
$$

$$
T_0^0 = \frac{\omega T^2}{r^2}\,(\alpha^2 + \beta^2)
$$

$$
T_1^1 = -\frac{\omega T^2}{r^2}\,(\alpha^2 + \beta^2) + 2\,\frac{T}{r^3}\,w\,\alpha\beta + \frac{mT}{r^2}\,(\alpha^2 - \beta^2)
$$

$$
T_2^2 = T_3^3 = -\frac{T}{r^3}\,w\,\alpha\beta \quad ,
$$

and all other components vanish. The normalization condition for the spinors is (as in [3]),

$$
\int_0^\infty (\alpha^2 + \beta^2)\,\frac{T}{\sqrt{A}} = 1 \quad . \tag{2.25}
$$

By substituting the formulas for the YM current and energy-momentum tensor into the Einstein and YM equations, we obtain the following system of ODEs,

$$
r\,A' = 1 - A - \frac{\kappa}{e^2}\frac{(1 - w^2)^2}{r^2} - 2\kappa\,\omega T^2(\alpha^2 + \beta^2) - \frac{2\kappa}{e^2}\,A\,w'^2 \tag{2.26}
$$

$$
2rA\,\frac{T'}{T} = -1 + A + \frac{\kappa}{e^2}\frac{(1 - w^2)^2}{r^2} + 2\kappa\,mT(\alpha^2 - \beta^2) - 2\kappa\,\omega\,T^2(\alpha^2 + \beta^2)
$$

$$
+ 4\kappa\,\frac{T}{r}\,w\,\alpha\beta - \frac{2\,\kappa}{e^2}\,A\,w'^2 \tag{2.27}
$$

$$
r^2 A\,w'' = -(1 - w^2)\,w + e^2\,rT\alpha\beta - r^2\,\frac{A'\,T - 2A\,T'}{2T}\,w' \quad . \tag{2.28}
$$

The Einstein equations are (2.26) and (2.27), whereas (2.28) is the YM equation. Our EDYM system is given by the five ODEs (2.23), (2.24), (2.26)–(2.28), together with the normalization condition (2.25).

We are interested here in bound states of the Dirac particles. Thus we want to find particle-like solutions of our EDYM system, i.e. solutions which are smooth and tend to the vacuum solution as $r \to \infty$. According to the explicit formulas (2.4)–(2.6), the energy-momentum tensor of the YM field is regular at $r = 0$ only when $|w(0)| = 1$ and $w'(0) = 0$. Using the remaining gauge freedom, we can assume that $w(0) = 1$, and thus

$$
w(r) = 1 - \frac{\lambda}{2}\,r^2 + \mathcal{O}(r^3) \tag{2.29}
$$

with a real parameter λ. Using this result, a local Taylor expansion of the Einstein and Dirac equations around $r = 0$ yields (just as in [3]) that

$$
\alpha(r) = \alpha_1\,r + \mathcal{O}(r^3) \quad , \qquad \beta(r) = \frac{1}{2}\,(\omega T_0 - m)\,\alpha_1\,r^2 + \mathcal{O}(r^3) \tag{2.30}
$$

$$
A(r) = 1 + \mathcal{O}(r^2) \quad , \qquad T(r) = T_0 + \mathcal{O}(r^2) \tag{2.31}
$$

with two parameters α_1 and $T_0 > 0$. Using linearity of the Dirac equation, we can always assume that $\alpha_1 > 0$. Furthermore, we demand that our solution has finite ADM mass,

$$
\rho := \lim_{r\to\infty} \frac{r}{2\kappa}(1 - A(r)) < \infty \quad , \tag{2.32}
$$

and goes asymptotically to the vacuum solution,

$$\lim_{r \to \infty} T(r) \;=\; 1 \quad , \qquad \lim_{r \to \infty} (w(r), w'(r)) \;=\; (\pm 1, 0) \quad , \qquad \lim_{r \to \infty} (\alpha(r), \beta(r)) \;=\; (0, 0) \quad . \tag{2.33}$$

3   The Reciprocal Coupling Limit

Under all realistic conditions, the coupling of Dirac particles to the YM field (describing the weak or strong interactions) is much stronger than the coupling to the gravitational field. Thus we are particularly interested in the case of weak gravitational coupling. In preparation, it is instructive to briefly consider the case without gravitation. In this limit, the Dirac equations read

$$\alpha' \;=\; \frac{w}{r}\,\alpha \;-\; (m + \omega)\,\beta \tag{3.1}$$

$$\beta' \;=\; (-m + \omega)\,\alpha \;-\; \frac{w}{r}\,\beta \quad . \tag{3.2}$$

For large r, these equations go over to a linear system of ODEs with constant coefficients, and the sign of $m - \omega$ determines whether the solutions of these equations behave oscillatory or exponentially. The normalization condition (2.25) excludes the oscillatory case (as in [6, Section 5]) and thus $m - \omega \geq 0$. In the case $m - \omega = 0$, the β-equation is independent of α, and the boundary conditions (2.30) imply that $\beta \equiv 0$. As a consequence, (2.28) reduces to the homogeneous YM equation

$$r^2\,w'' \;=\; -(1 - w^2)\,w \quad . \tag{3.3}$$

It is well-known [7] that the only solution to this equation satisfying the boundary conditions (2.29),(2.33) is the trivial solution $w \equiv 1$. But then the α-equation simplifies to

$$\alpha' \;=\; \frac{1}{r}\,\alpha \quad ,$$

whose solution $\alpha = \alpha_1 r$ violates the normalization condition (2.25). In the case $m - \omega > 0$, on the other hand, the local Taylor expansion (2.30) yields that the (α, β)-curve lies for small r in the fourth quadrant, i.e. $\beta(r) < 0 < \alpha(r)$ for small r. Using the Dirac equations (3.1),(3.2), one sees that the fourth quadrant is an invariant region, and thus $\beta(r) < 0 < \alpha(r)$ for all r. But in the fourth quadrant, both $\alpha(r)$ and $-\beta(r)$ are increasing for large r (as one sees in (3.1),(3.2) taking into account that $w/r \to 0$ for $r \to \infty$), and thus the normalization condition (2.25) will again be violated.

These considerations show that the gravitational field is essential for the formation of bound states. Nevertheless, for arbitrarily weak gravitational coupling, we can hope to find bound states. It is even conceivable that these bound state solutions might have a well-defined limit when the gravitational coupling tends to zero, if we let the YM coupling go to infinity at the same time. Our idea is that this limiting case might yield a system of equations which is simpler than the full EDYM system, and can thus serve as a physically interesting starting point for the analysis of the coupled interactions described by the EDYM equations. Expressed in dimensionless quantities, we shall thus consider the limits

$$m^2 \kappa \;\to\; 0 \qquad \text{and} \qquad e^2 \;\to\; \infty \quad . \tag{3.4}$$

Let us determine how the quantities of our EDYM system should behave in this limit. Since we are considering weak gravitational coupling, it is clear that the metric will be close to the Minkowski metric, i.e. $A \approx 1$ and $T \approx 1$. Furthermore, the YM potential w should have a finite limit. Similar to our flat space consideration at the beginning of this section, one sees that the normalization condition (2.25) can be satisfied only if the function $m - \omega T(r)$ changes sign, and thus $\omega \approx m$ (but both m and ω may go to zero or infinity in the limit (3.4)). Putting this information together, we conclude that the Dirac equations (2.23) and (2.24) have a meaningful limit only under the assumptions that α converges and that

$$m\,\beta(r) \;\to\; \hat{\beta}(r) \quad , \qquad m^2\,(T(r) - 1) \;\to\; \varphi \quad , \qquad m\,(\omega - m) \;\to\; E \qquad (3.5)$$

with two real functions $\hat{\beta}$, φ and a real parameter E. Multiplying (2.24) with m and taking the limits (3.5) as well as $A, T \to 1$, the Dirac equations become

$$\alpha' \;=\; \frac{w}{r}\,\alpha \;-\; 2\,\hat{\beta} \qquad (3.6)$$

$$\hat{\beta}' \;=\; (E + \varphi)\,\alpha \;-\; \frac{w}{r}\,\hat{\beta} \quad . \qquad (3.7)$$

We next consider the YM equation (2.28). The last term in (2.28) drops out in the limit of weak gravitational coupling (3.4). The second summand converges only under the assumption that

$$\frac{e^2}{m} \;\to\; q \qquad (3.8)$$

with q a real parameter, playing the role of an "effective" coupling constant. Together with (3.4), this implies that $m \to \infty$. The YM equations thus have the limit

$$r^2\,w'' \;=\; -(1 - w^2)\,w \;+\; q\,r\,\alpha\hat{\beta} \quad . \qquad (3.9)$$

In order to get a well-defined and non-trivial limit of the Einstein equations (2.26),(2.27), we need to assume that the parameter $m^3\kappa$ has a finite, non-zero limit. Since this parameter has the dimension of inverse length, we can arrange by a scaling of our coordinates that

$$m^3\kappa \;\to\; 1 \quad . \qquad (3.10)$$

We differentiate the T-equation (2.27) with respect to r and substitute (2.26). Taking the limits (3.5) and (3.10), a straightforward calculation yields the equation

$$r^2\,\Delta\varphi \;=\; -\alpha^2 \quad , \qquad (3.11)$$

where $\Delta = r^{-2}\partial_r(r^2\partial_r)$ is the radial Laplacian in Euclidean $\mathrm{I\!R}^3$. Indeed, this equation can be regarded as Newton's equation with the Newtonian potential φ. Thus our limiting case (3.11) for the gravitational field corresponds to taking the Newtonian limit. Finally, the normalization condition (2.25) reduces to

$$\int_0^\infty \alpha(r)^2\,dr \;=\; 1 \quad . \qquad (3.12)$$

The boundary conditions (2.29)–(2.33) are transformed into

$$w(r) \;=\; 1 \;-\; \frac{\lambda}{2}\,r^2 \;+\; \mathcal{O}(r^3) \quad , \qquad \lim_{r\to\infty} w(r) \;=\; \pm 1 \qquad (3.13)$$

$$\alpha(r) \;=\; \alpha_1\,r \;+\; \mathcal{O}(r^3) \qquad , \qquad \hat{\beta}(r) \;=\; \mathcal{O}(r^3) \qquad (3.14)$$

$$\varphi(r) \;=\; \varphi_0 \;+\; \mathcal{O}(r^2) \qquad , \qquad \lim_{r\to\infty} \varphi(r) \;<\; \infty \qquad (3.15)$$

with the three parameters λ, α_1, and φ_0. We point out that the limiting system contains only one coupling constant q. According to (3.8) and (3.10), q is in dimensionless form given by

$$e^2\, m^2 \kappa \;\to\; q \quad . \tag{3.16}$$

Hence in dimensionless quantities, our limit (3.4) describes the situation where the gravitational coupling goes to zero, while the YM coupling constant goes to infinity like $e^2 \sim (m^2\kappa)^{-1}$. Therefore, we call our limiting case the *reciprocal coupling limit*. The reciprocal coupling system is given by the equations (3.6), (3.7), (3.9), and (3.11) together with the normalization condition (3.12) and the boundary conditions (3.13)–(3.15). According to (3.5), the parameter E coincides up to a scaling factor with $\omega - m$, and thus has the interpretation as the (properly scaled) energy of the Dirac particle. As in Newtonian mechanics, the potential φ is determined only up to a constant $\mu \in \mathbb{R}$; namely, the reciprocal limit equations are invariant under the transformation

$$\varphi \;\to\; \varphi + \mu \quad , \qquad E \;\to\; E - \mu \quad . \tag{3.17}$$

Let us consider how the ADM mass behaves in the reciprocal coupling limit. First of all, we can write the quotient ρ/m as

$$\frac{\rho}{m} \;=\; \lim_{r\to\infty} \frac{r}{2\kappa m}\,(1 - A(r)) \;=\; \frac{1}{m}\int_0^\infty \left(\frac{r}{2\kappa}\,(1 - A(r))\right)' dr \quad .$$

After substituting the A-equation (2.26), we can take the limits (3.4) and (3.5) and obtain that

$$\frac{\rho}{m} \;\to\; \int_0^\infty \alpha(r)^2\, dr \;\overset{(3.12)}{=}\; 1 \quad . \tag{3.18}$$

Thus the ADM mass coincides with the rest mass of the Dirac particle; this shows that the total binding energy $B := \rho - m$ goes to zero in our limit. Indeed, the behavior of the total binding energy can be described in more detail as follows. For a solution of the full EDYM system, we can write the binding energy using the normalization condition (2.25) as

$$B \;=\; \int_0^\infty \left(\left(\frac{r}{2\kappa}\,(1 - A)\right)' - m\,(\alpha^2 + \beta^2)\,\frac{T}{\sqrt{A}}\right) dr \quad .$$

We again substitute the A-equation (2.26) and obtain

$$B \;=\; \int_0^\infty \left(\frac{1}{2e^2}\,\frac{(1 - w^2)^2}{r^2} \;+\; \frac{1}{e^2}\,A w'^2 \;+\; (w T\sqrt{A} - m)\,\frac{T}{\sqrt{A}}\,(\alpha^2 + \beta^2)\right) dr \quad . \tag{3.19}$$

According to (3.16), it is obvious that the first two summands in (3.19) have a finite limit after dividing by $m^2\kappa$. In order to treat the last summand, we first multiply the T-equation (2.27) with m^2 and take the limits (3.4), (3.5), (3.10),

$$m^2\,(A - 1) \;\to\; 2r\,\varphi' \quad .$$

Using again (3.10), (3.5), and $\omega \to m$, $T \to 1$, we obtain that

$$\begin{aligned}
\frac{1}{m^2\kappa}\,(\omega T\sqrt{A} - m) \;&=\; \frac{1}{m^3\kappa}\,m\omega\,(\sqrt{A} - 1)\,T \;+\; \frac{1}{m^3\kappa}\,m(\omega T - m)\\
&\to\; r\varphi' + (\varphi + E) \quad .
\end{aligned}$$

9

From this we conclude that the binding energy (3.19) divided by $m^2 \kappa$ has a meaningful limit; more precisely

$$\hat{B} \ := \ \frac{B}{m^2 \kappa} \ \to \ \int_0^\infty \left(\frac{1}{2q} \frac{(1-w^2)^2}{r^2} \ + \ \frac{1}{q} \, w'^2 \ + \ \alpha^2 \, (E + \varphi + r\varphi') \right) dr \quad . \qquad (3.20)$$

We now describe our method for constructing numerical solutions of our reciprocal limit system. Since it is difficult to take into account the integral condition (3.12) in the numerics, we discard this condition for the construction of the solution; it will be taken care of later via a rescaling technique (see (3.34), (3.35)). This rescaling method requires only that the normalization integral be finite,

$$0 \ < \ \lambda^2 := \int_0^\infty \alpha(r)^2 \, dr \ < \ \infty \quad . \qquad (3.21)$$

According to (3.6), (3.7) and (3.13), (3.15), the behavior of the Dirac spinors at infinity is either oscillatory or exponential. As a consequence, the normalization integral in (3.21) will be finite only if $\alpha(r)$ tends to zero for $r \to \infty$. Furthermore, we can use the transformation (3.17) to set $\varphi(0) = 0$. Hence in the first construction step, we want to find solutions of the modified system

$$\alpha' \ = \ \frac{w}{r} \, \alpha \ - \ 2 \, \hat{\beta} \qquad (3.22)$$

$$\hat{\beta}' \ = \ (E + \varphi) \, \alpha \ - \ \frac{w}{r} \, \hat{\beta} \qquad (3.23)$$

$$r^2 \, w'' \ = \ -(1 - w^2) \, w \ + \ q \, r \, \alpha \hat{\beta} \qquad (3.24)$$

$$r^2 \, \Delta\varphi(r) \ = \ -\alpha^2 \qquad (3.25)$$

with the following conditions at the origin,

$$w(r) \ = \ 1 - \lambda r^2 + \mathcal{O}(r^3) \quad , \qquad \alpha(r) \ = \ \alpha_1 \, r + \mathcal{O}(r^2) \qquad (3.26)$$

$$\varphi(r) \ = \ \mathcal{O}(r^2) \qquad \qquad , \qquad \beta(r) \ = \ \mathcal{O}(r^3) \quad , \qquad (3.27)$$

together with the conditions at infinity

$$\lim_{r \to \infty} w(r) \ = \ \pm 1 \quad , \qquad \lim_{r \to \infty} \alpha(r) \ = \ 0 \qquad (3.28)$$

$$|\varphi_\infty| := |\lim_{r \to \infty} \varphi(r)| \ < \ \infty \quad . \qquad (3.29)$$

For any given value of the coupling constant q, we thus have two free parameters λ and α_1 to characterize the solutions near the origin $r = 0$. Each solution has a unique extension to larger values of r. Asymptotically for $r \to \infty$, we must satisfy the two conditions (3.28). Thus we have as many free parameters as asymptotic conditions, and we therefore expect for fixed q a discrete set of solutions satisfying (3.26), (3.27), and (3.28). For each solution, we must then verify that the conditions (3.21) and (3.29) are also satisfied.

For the construction of numerical solutions, we enhanced the technique used in [3, 4] to a two-parameter shooting method. Since two-parameter problems are considerably more difficult than one-parameter problems, we describe the method in some detail. For clarity, we first consider the simplified situation where $\alpha(r)$ and $w(r)$ have prescribed boundary values for a given finite $r = r_1$. In this case, one can apply the standard multi-parameter

shooting method as e.g. described in [8]. More precisely, one can for given initial data compute $\alpha(r_1)$ and $(w(r_1), w'(r_1))$ numerically, compare with the prescribed boundary conditions, and iteratively adjust the two free parameters λ and α_1 until the boundary conditions are satisfied to sufficient accuracy. In our case, the situation is more difficult because we have boundary values not for finite $r = r_1$, but for $r = \infty$. In order to deal with this problem, we first choose a finite r_1. Using an ansatz for the asymptotic form of the solution $(\alpha, \hat{\beta}, w, \varphi)$ at infinity, we approximately compute $\alpha(r_1)$ and $(w(r_1), w'(r_1))$ and derive conditions between these functions. Taking these conditions as the boundary conditions at $r = r_1$, we can apply the two-parameter shooting method on the finite interval $(0, r_1]$ as described above. The so-obtained solution on $(0, r_1]$ gives, in combination with the asymptotic formulas on (r_1, ∞), an approximate solution for all $r > 0$. Since our asymptotic description becomes precise only in the limit $r_1 \to \infty$, we must, in order to attain the desired accuracy, choose r_1 sufficiently large. In order to ensure that r_1 is appropriately increased during the computation, we modified the two-parameter shooting method in such a way that both the initial data and r_1 are adjusted in each iteration step. The iteration is stopped when the numerics has stabilized and the accuracy no longer improves. This modified shooting method was implemented in the Mathematica programming language using the standard ODE solver with a working precision of 16 digits. The initial data is adjusted in the iteration with a secant method, and the step size for incrementing r_1 is determined from the relative error of the numerical solution at the upper boundary r_1. After the iteration has been stopped and a numerical solution has been found, our program slightly changes the initial data and searches for a nearby solution. In this way, we can automatically trace a one-parameter family of solutions. Finally, we explain our method for describing the asymptotic behavior of the solutions at infinity. According to the asymptotics of the solutions of the ED and EYM equations [3, 1], we can expect that the spinors α and $\hat{\beta}$ will decay exponentially fast at infinity, whereas the potentials $\varphi(r)$ and $w(r)$ for $r \to \infty$ will behave like rational functions. Therefore it is a reasonable asymptotic approximation to set α and $\hat{\beta}$ to zero for $r > r_1$. In this approximation, the potential φ is harmonic according to (3.25). The YM equation (3.24), on the other hand, reduces to the vacuum YM equation (3.3). In the new variable $u = \log r$, this equation becomes autonomous; namely [7]

$$\partial_u^2 w - \partial_u w \;=\; -(1 - w^2)\, w \quad . \tag{3.30}$$

This autonomous equation allows us to derive boundary conditions for w as follows. We set

$$x = w \qquad \text{and} \qquad y = \partial_u w \quad . \tag{3.31}$$

Then the YM orbits in the (x, y) plane are described by the following differential equation,

$$y'(x) \;=\; \frac{\partial_u^2 w}{\partial_u w} \overset{(3.30)}{=} 1 - \frac{(1 - x^2)\, x}{y} \quad . \tag{3.32}$$

According to the boundary conditions (3.28) and the differential equation (3.30), the variables x and y must behave in the limit $r \to \infty$ like either $x \to 1$, $y \searrow 0$ or $x \to -1$, $y \nearrow 0$. In both of these cases, there is a unique YM orbit $y(x)$, which can be easily calculated numerically by integrating (3.32). By transforming (3.31) back to the variable r, we obtain the following mixed boundary conditions for $w(r)$ at $r = r_1$,

$$w'(r_1) \;=\; \frac{1}{r_1}\, y(w(r_1)) \quad . \tag{3.33}$$

We next describe our rescaling method needed to arrange the normalization condition (3.12). Suppose that we have a solution of the modified system (3.22)–(3.29) with finite normalization integral, (3.21). A direct calculation shows that the transformed functions

$$\tilde{\alpha}(r) \;=\; \lambda^{-2}\,\alpha(\lambda^{-2}r) \qquad , \qquad \tilde{\tilde{\beta}}(r) \;=\; \lambda^{-4}\,\beta(\lambda^{-2}r) \qquad (3.34)$$

$$\tilde{\varphi}(r) \;=\; \lambda^{-4}\left(\varphi(\lambda^{-2}r) - \varphi_\infty\right) \quad , \qquad \tilde{w}(r) \;=\; w(\lambda^{-2}r) \qquad (3.35)$$

solve our original reciprocal limit system (3.6), (3.7), (3.9), (3.11), and (3.12) with boundary conditions (3.13)–(3.15), if one replaces the energy E and coupling constant q by

$$\tilde{E} \;=\; \lambda^{-4}\,(E + \varphi_\infty) \qquad \text{and} \qquad \tilde{q} \;=\; \lambda^4\,q \quad . \qquad (3.36)$$

We point out that only the rescaled solutions (3.34),(3.35) and rescaled parameters (3.36) have a physical meaning. Therefore, we will in what follows consider only the rescaled tilde solutions; for ease in notation, the tilde will be omitted.

In the remainder of this section, we describe our numerical solutions of the reciprocal limit equations. Just as in the case for the ED and EYM equations [3, 1], there are solutions for different rotation numbers of the spinors in the (α, β)-plane and for the YM potential in the (w, w')-plane. For simplicity, we restricted attention to solutions with rotation number zero for the spinors (as for the ground state solutions in [3]). For the YM potential, we consider only the cases where the (w, w')-curve either makes a half rotation joining the points $(1, 0)$ and $(-1, 0)$, or makes a full rotation, ending at its starting point $(1, 0)$. A typical example for a solution of each type is shown in Figures 1 and 2. Because of the similarity of the YM potential to the BM ground state and the BM first excited state, we refer to these two types in what follows as the ground states and the first excited states, respectively. Notice that the curves in the (w, w')-plane are not plotted all the way to their rest points at $(1, 0)$ or $(0, -1)$, respectively. The reason is that we plot only the numerical solution on the interval $(0, r_1]$. One sees that the spinors have become practically zero for $r = r_1$, and it is thus an admissible approximation to smoothly join the (w, w')-curve with a vacuum YM solution by using the boundary conditions (3.33). We first discuss the ground state solutions. In Figure 3, the main characteristics of the solutions are plotted versus the coupling constant q. As explained above, E has the interpretation of the (appropriately scaled) energy of the Dirac particle. Since E is negative, the Dirac particle has gained energy by forming the bound state. The parameter $\hat{B}$, (3.20), gives the total binding energy, i.e. the amount of energy which is set free when the binding is broken up. Since $\hat{B}$ is negative, we can expect that solutions of the full EDYM system, which are close to the solutions of the reciprocal coupling equations, should be stable. Finally, r_w and r_α are the characteristic length scales of the solutions; more precisely, r_w is the radius where w changes sign, and r_α is the radius where α has its maximum,

$$w(r_w) \;=\; 0 \qquad \text{and} \qquad \alpha'(r_\alpha) \;=\; 0 \quad . \qquad (3.37)$$

The characteristic radii are interesting because they give information about the "size" of the solutions as functions of r; i.e. they tell whether the fields are spread out in space, or whether they are localized close to the origin. It is also worth considering both radii because r_w and r_α can behave quite differently (cf. Figure 3).

The plots in Figure 3 have a turning point at $q \approx 8.49$. Similar to the situation described for the spiral in [3], this is a bifurcation point which comes about as a consequence

of our rescalings. One branch of solutions can be extended up to $q \approx 11.6$. For solutions close to this end point, the potential w leaves the interval $[-1, 1]$ as shown in Figure 4. Since r_w and r_α both go to zero in this limit, the spinors and YM field are both confined to a smaller and smaller neighborhood of the origin. At the same time, the energy of the Dirac particle and the binding energy become infinite. The other branch of solutions ends near $q = 8.95$. For solutions near this end point, the (w, w')-curve comes very close to the origin before running into the rest point at $(-1, 0)$, see Figure 5. This makes the numerics rather delicate, and we therefore have not yet analyzed this regime in much detail. It is interesting that r_α is bounded near this end point, whereas r_w seems to become infinite. This shows that, while the Dirac particle stays in a bounded region of space, the YM field becomes more and more spread out.

For the first excited state, the energy spectrum and characteristic radii are shown in Figure 6. Since in general w never equals zero for the first excited state, we define r_w via the minimum of w, i.e.

$$w'(r_w) \;=\; 0 \qquad \text{and} \qquad \alpha'(r_\alpha) \;=\; 0 \;\;. \tag{3.38}$$

In contrast to the ground state, the solutions can now be extended up to $q = 0$. In this regime, the YM potential stays close to $w = 1$; see Figure 7. The solutions have a bifurcation point at $q \approx 9.866$. The branch coming out at the bifurcation point for larger values of E is difficult to study numerically because the (w, w')-curve comes close to the origin, see Figure 8.

It is interesting that for the ground state solutions in Figure 3, the parameter q stays bounded away from zero, whereas the plots for the first excited state in Figure 6 could be extended up to $q = 0$. Let us consider how this can be understood directly from the equations. The parameter q enters only the YM equation (3.9). In the limit $q \to 0$, this equation goes over to the vacuum YM equation, which has only the trivial solution $w \equiv 1$. Hence if we assume that the spinors have a finite limit for $q \to 0$, then $w(r)$ must go uniformly in r to one. This shows that the solutions can be regular for $q \to 0$ only if w satisfies the boundary condition $\lim_{r \to \infty} w(r) = +1$. In particular, our ground state solutions cannot be regular in this limit. We next consider the limit $q \to 0$ for the first excited state in more detail. Since w converges uniformly in r to one, the reciprocal limit equations (3.6), (3.7), and (3.11) go over to the Dirac-Newton equations

$$\alpha' \;=\; \frac{1}{r}\,\alpha \,-\, 2\,\hat{\beta} \tag{3.39}$$

$$\hat{\beta}' \;=\; (E + \varphi)\,\alpha \,-\, \frac{1}{r}\,\hat{\beta} \tag{3.40}$$

$$r^2\,\Delta\varphi(r) \;=\; -\alpha^2 \;\;. \tag{3.41}$$

These equations are obtained by taking the nonrelativistic limit of the ED equations [3], and according to the results obtained in that paper, the equations (3.39)–(3.41) together with the normalization integral (3.12) have a countable number of solutions, characterized by the rotation number of the spinors (called the ground state, the first excited state, etc.). We thus expect that the functions $(\alpha, \hat{\beta}, \varphi)$ corresponding to solutions of the reciprocal limit equations should for $q \to 0$, go over to a solution of the Dirac-Newton equations. The behavior of the YM potential w can now be analyzed in more detail by taking the solution $(\alpha, \hat{\beta}, \varphi)$ of the Dirac-Newton equations as a given inhomogeneity in the YM equation (3.9) and performing a perturbation calculation for small q. More precisely, the ansatz

$w(r) = 1 + q\,u(r)$ to first order in q, leads to the linear equation

$$r^2\,u'' \;=\; 2u \,+\, r\,\alpha\hat{\beta} \quad,$$

which can be solved by integration. Fixing the integration constants with our boundary conditions $u(0) = u(\infty) = 0$ and $u'(0) = 0$, we obtain the unique solution

$$u(r) \;=\; r^2 \int_0^r \frac{ds}{s^4} \int_0^s t\,\alpha(t)\,\hat{\beta}(t)\,dt \;-\; \frac{r^2}{3} \int_0^\infty \frac{1}{t^2}\,\alpha(t)\,\hat{\beta}(t)\,dt \quad. \tag{3.42}$$

This consideration shows that for $q \to 0$, the rotation number of w is uniquely determined by the rotation number of the spinors. Furthermore, one sees that in the limit $q \to 0$, the Dirac wave function is determined by the Dirac-Newton equations (3.39)–(3.41). Thus only the gravitational attraction is responsible for the formation of the bound state, whereas the YM field has no influence on the spinors.

4 Solutions of the EDYM Equations

In this section, we shall construct numerical solutions of the full EDYM equations and discuss their properties. Our method is to first find special solutions which are small perturbations of either the BM solutions [1] or solutions to the reciprocal limit equations of the previous section. We then trace these solutions while gradually changing the coupling constants. This yields one-parameter families of solutions which can be extended even to regions in parameter space where the solutions are far from all of the known limiting cases.

In order to simplify the connection between the EDYM equations and the reciprocal limit equations of Section 3, it is useful to introduce a parameter $\varepsilon > 0$ in such a way that the reciprocal limit equations are obtained when $\varepsilon \to 0$. To this end, we parametrize the EDYM equations in terms of the new variables (ε, q, E) as follows,

$$\kappa \;=\; (\varepsilon q)^{\frac{3}{2}} \quad, \qquad e^2 \;=\; \sqrt{\frac{q}{\varepsilon}}$$

$$m \;=\; \frac{1}{\sqrt{\varepsilon q}} \quad, \qquad \omega \;=\; \frac{1}{\sqrt{\varepsilon q}} \,+\, \sqrt{\varepsilon q}\,E \quad.$$

Since the EDYM equations involve three dimensionless parameters (namely $m^2\kappa$, ω/m, and e^2), introducing (ε, q, E) is merely a transformation to new independent parameters, prescribing at the same time the gravitational constant (this means that we give up the freedom to rescale r by fixing our length scale). In the limit $\varepsilon \to 0$, both q and E go over to the corresponding parameters of the reciprocal limit system (see (3.8) and (3.5)). Also, it is easy to check that the limits (3.4), (3.10), and (3.16) are satisfied if we let $\varepsilon \to 0$ and keep (q, E) fixed. The parameters ε and q can be written in dimensionless form as

$$\varepsilon \;=\; \frac{m^2\kappa}{e^2} \quad, \qquad q \;=\; m^2\kappa\,e^2 \quad. \tag{4.1}$$

Thus ε describes the relative strength of gravity versus the YM interaction, whereas q is the product of the gravitational and YM coupling constants. Up to a scale factor, $E = \omega - m$. Since ω is the relativistic energy and m the rest mass of the Dirac particle, E can, exactly as in the previous section, be interpreted as the energy of the Dirac particle.

Finally, we also describe the binding energy by a parameter which corresponds to our notation for the reciprocal limit system (3.20) and set

$$\hat{B} = \frac{\rho - m}{\sqrt{\varepsilon q}} \quad .$$

For the construction of numerical solutions, we use a two-parameter shooting algorithm combined with a rescaling method. Since this technique is quite similar to that described for the reciprocal limit equations in the previous section, we shall merely outline our procedure. In the first step of the construction, we consider the EDYM equations (2.23), (2.24) and (2.26)–(2.28) with the side conditions

$$0 < \lambda^2 := \int_0^\infty (\alpha^2 + \beta^2) \frac{T}{\sqrt{A}} \, dr < \infty \tag{4.2}$$

$$0 < \tau := \lim_{r \to \infty} T(r) < \infty \tag{4.3}$$

$$\lim_{r \to \infty} w(r) = \pm 1 \quad , \tag{4.4}$$

together with the following expansions near $r = 0$,

$$\begin{aligned}
\alpha(r) &= \alpha_1 r + \mathcal{O}(r^3) \quad , & \beta(r) &= \mathcal{O}(r^2) \\
A(r) &= 1 + \mathcal{O}(r^2) \quad , & T(r) &= 1 + \mathcal{O}(r^2) \quad .
\end{aligned}$$

For fixed ε and q, we thus have the two parameters α_1 and E to characterize a solution of this modified EDYM system near the origin $r = 0$. On the other hand, we must satisfy two conditions at infinity; namely, w must converge to ± 1, (4.4), and the spinors must go asymptotically to zero in order for the normalization integral to be finite (4.2). Hence, we can apply a two-parameter shooting method as described in Section 3. In order to have optimal boundary conditions at the upper end point $r = r_1$, we again match this with the solution of the autonomous vacuum YM equation (see (3.32) and (3.33)). The shooting method was again implemented in Mathematica, using an accuracy of 32 digits. For each solution constructed in this way, we verify that (4.3) is satisfied and that the ADM mass is finite (2.32). Once we have found a solution of the modified equations, we rescale the solution according to

$$\begin{aligned}
\tilde{\alpha}(r) &= \sqrt{\tau}\, \lambda^{-2} \, \alpha(\lambda^{-2} r) \quad , & \tilde{\beta}(r) &= \sqrt{\tau}\, \lambda^{-2} \, \beta(\lambda^{-2} r) \tag{4.5} \\
\tilde{A}(r) &= A(\lambda^{-2} r) \quad , & \tilde{T}(r) &= \tau^{-1} \, T(\lambda^{-2} r) \quad , \tag{4.6}
\end{aligned}$$

and transform the parameters (m, ω, κ, e^2) as follows,

$$\begin{aligned}
\tilde{m} &= \lambda^{-2} m \quad , & \tilde{\omega} &= \tau\, \lambda^{-2}\, \omega \tag{4.7} \\
\tilde{\kappa} &= \lambda^6 \kappa \quad , & \tilde{e}^2 &= \lambda^2 e^2 \quad . \tag{4.8}
\end{aligned}$$

A straightforward calculation shows that the so-rescaled solution satisfies the EDYM equations (2.23), (2.24) and (2.26)–(2.28) together with the original side conditions (2.25) and (2.30)–(2.33). The parameters (ε, q, E) transform under the rescalings as

$$\tilde{\varepsilon} = \varepsilon \quad , \quad \tilde{q} = \lambda^4 q \quad , \quad \tilde{E} = \lambda^{-4} \left(E + (\tau - 1)\, m\omega \right) \quad . \tag{4.9}$$

In the limit $\varepsilon \to 0$, these transformations coincide with the rescalings of the reciprocal limit equations (3.34)–(3.36). However, we remark that for the ED equations [3] a much

different rescaling is used. Namely, in order to get a better correspondence to the reciprocal limit equations, we here scale the gravitational constant κ, whereas in [3] κ is fixed to be 1 throughout. Clearly, only the rescaled solutions have physical significance. Therefore, in what follows we will consider only the rescaled solutions and again omit the tilde.

In a realistic physical situation, the gravitational coupling is very weak, whereas the YM coupling constant is of order one, i.e. $m^2\kappa \ll 1$ and $e^2 \sim 1$. Hence, according to (4.1), we will here only investigate the parameter range $\varepsilon \ll 1$, and we are particularly interested in the situation for small q. In the limit $\varepsilon \to 0$, there are known solutions of our EDYM system, namely the BM solutions (which more precisely are solutions in the limits $\kappa \to 0$ and $e^2/\kappa \to 1$), and the solutions of the reciprocal limit system constructed in Section 3. We take these special solutions as the starting point for the numerics. By varying the parameters ε and q and tracing the solutions with our shooting and rescaling methods, we obtain a two-parameter family of solutions. In order to reduce the computational workload, we did not step systematically through the two-parameter space, but always kept one parameter fixed while varying the other parameter. Since ε remains unchanged under the rescaling (see (4.9)), it is most convenient to construct one-parameter families of solutions for different, fixed values of ε.

We now describe the solutions we found. Exactly as for the reciprocal limit system in Section 3, we restricted attention to solutions with rotation number zero for the spinors and a rotation angle of π or 2π for the YM potential. We again refer to these types of solutions as the "ground state" and the "first excited state," respectively. For the ground state solutions, the energy spectrum and the characteristic radii are in Figures 9 and 10 plotted for different values of the parameter ε (the characteristic radii are again defined by (3.37)). The curves A for $\varepsilon = 0$ coincide with the plots for the reciprocal limit system in Figure 3. For small values of the parameter ε, there are solutions for the EDYM equations which are close to the solutions of the reciprocal limit equations (compare the curves A and B in Figure 9). In this parameter regime, the EDYM solutions look typically as shown in Figure 11. The metric functions A and T are both close to one; thus the gravitational interaction is weak, in agreement with our considerations after (3.4). The spinors and the YM potential look very similar to the solution of the reciprocal limit equations in Figure 5. *We conclude that the reciprocal limit system of Section 3 indeed describes a significant limiting case of the EDYM equations.* However, one also sees that even for small ε, not all the solutions of the EDYM equations are close to the reciprocal limit solutions. More precisely, curve B leaves the vicinity of curve A at $q \approx 10$ (see Figure 10). If one follows curve B after it branches off from curve A, the parameter q first increases up to a turning point, and then decreases to $q = 0$. If ε gets large, the solution curves no longer come so close to the reciprocal limit solutions (see curves C and D). The maximum of q decreases (see curve C) and finally disappears (see curve D). Figure 12 shows a typical solution for small q. We note that in this parameter region, the metric functions A and T are not near one; this explains why the reciprocal limit equations are no longer a good approximation. Indeed, the potentials w, A, and T now resemble a BM solution of the EYM equations [1], and the spinors look like the solution of the Dirac equation in the BM background. Hence $q \to 0$ corresponds to the limit of weakly coupled spinors; i.e. spinors in a fixed BM background. Notice that the characteristic radii go to zero and the energies go to infinity in the limit $q \to 0$ (see Figure 9). This can be understood from our rescalings. Namely, for the (unscaled) solutions of our modified EDYM system, the BM solutions are easily obtained by taking the limit $\alpha_1 \to 0$ (in which the spinors go uniformly in r to zero). In this limit, the normalization integral (4.2) tends to zero, and thus the rescalings (4.5)–

(4.9) lead to a singular behavior of the rescaled solutions for $q \to 0$. To summarize, there is a one-parameter family of solutions (obtained by continuously changing the coupling constants), connecting the BM solutions to our reciprocal limit solutions

We remark that our plots of the curves B have a small gap at $q \approx 8.7$. The reason is that in this region the numerics become unstable, and could not be carried out with our methods. But we were able to construct two branches of solutions which approach the problematic region from both sides. We suspect that the instability of the numerics is merely an artifact of our rescaling method, but it might well be an indication for a possible bifurcation point in this region. For the other curves C and D, we analyzed only the branch of solutions which extends towards smaller values of q.

For the first excited state, the energy spectrum and characteristic radii are plotted in Figures 13 and 14 (the characteristic radii are again defined by (3.38)). The curves A for $\varepsilon = 0$ correspond to the solutions of the reciprocal limit equations in Figure 6. In contrast to the situation for the ground state, the solutions for small ε are all close to the reciprocal limit solutions (compare the curves A and B). Figure 15 shows a typical solution for large q; one sees that the spinors and YM potential look similar to those in Figure 8. The form of the energy spectrum and the characteristic radii gradually change when ε is increased; for example, the cusp in the (q, r_w)-plot becomes smooth (see curve D). It is interesting that for $q \to 0$, the curves converge independent of ε to a single limit point (see Figure 13). This limit point was already described at the end of Section 3 as the case when the spinors form a bound state due to their gravitational attraction, and the spinors generate a YM field (see (3.39)–(3.42)). This picture is in agreement with our numerics, since the spinors and metric functions, for a solution near this limit point, look similar to the ED solutions [3] in the Newtonian limit, and $w \approx 1$ (see Figure 16). The fact that this limit point is independent of ε follows, because as explained at the end of Section 3, for $q \to 0$, the YM equation decouples from the ED equations. For clarity, we point out that it would not be correct to say that the gravitational interaction dominates the YM interaction in the limit $q \to 0$. Namely, according to (4.1), the ratio of the gravitational and YM coupling constants is kept fixed, and thus $q \to 0$ corresponds to the limit where both coupling constants go to zero at the same rate. Nevertheless, the YM field has for $q \to 0$ no influence on the energy spectrum and the characteristic radii.

A main qualitative difference between the ground state and the first excited state is that for the first excited state, we could not continuously join the solutions of the reciprocal limit equations with a BM solution. In order to see how this comes about, we did numerical calculations starting with a Dirac particle in the BM background (similar to that shown in Figure 17) and gradually increased the coupling of the spinors to gravity and to the YM field. For these "deformations of the first excited BM state," the curves of the energy spectrum and the characteristic radii have spirals, whose size and shape drastically changes when ε is increased, see Figures 18 and 19. In the parameter regime where the energy plots spiral around, the spinors have self-intersections similar as observed for the ED solutions [3], see Figure 20.

We now discuss the stability of our solutions. The relevant parameter for the stability analysis is the total binding energy $\hat{B}$. Namely, if $\hat{B}$ is negative and smaller than the total energies of all other states, then energy is needed to break up the binding or to make a transition to any of the other states, and therefore for physical reasons the solution must be stable. Clearly, this energy argument does not provide a rigorous stability proof, and it also cannot replace the numerical analysis of linear stability (like e.g. in [2] or [3, Section 8]), but it gives a strong indication for stability and is therefore commonly used

(see e.g. [9]). Let us first apply this energy argument to the ground state solutions of Figures 9 and 10. One sees that the total energy becomes negative for large q. For the curves B and C, this region is plotted in more detail in Figure 21. For the solutions on branch b, the total binding energy is minimal, and thus this branch is stable. Applying Conley index methods with q as the bifurcation parameter (see [10]), we obtain, as in [3], that the two other branches a and c are unstable. Indeed, the instability of branch c follows also from the continuity of the Conley index and the fact that in the limit $q \to 0$, this branch goes over to the ground state BM solution which is known to be unstable [2]. When ε is increased (see curve D, Figures 9 and 10), only one branch of solutions remains, which comprises the BM solutions as a limiting case and is therefore unstable. More precisely, the one-parameter family has in this case no bifurcation points, and in the limit $q \to 0$ the solutions tend to an unstable BM solution. Thus using Conley index techniques, it follows that the entire one-parameter family is unstable. We conclude that *for small ε, there is a stable branch of ground state solutions for which q lies in a finite interval away from $q = 0$*; all other ground state solutions are unstable. For the stability of the first excited state, we consider the plots of Figures 13 and 14. Since for $q \to 0$, the spinors and metric functions go over to the Newtonian limit of the ED solutions, we conclude from [3] that *the branch of solutions starting at $q = 0$ should be stable*. This is in agreement with our above energy argument, because on this branch the total binding energy $\hat{B}$ is negative, and is smaller than the total binding energy of the second branch of solutions, which comes out of the bifurcation point located at the maximum of q. Again, Conley index theory yields that this second branch is unstable. For the deformations of the first excited BM state, the total binding energy is positive (see Figures 19 and 20), and hence these solutions should be unstable. Indeed, for the branch of solutions which extends up to $q = 0$ (i.e. before the first bifurcation point), this also follows from the continuity of the Conley index and the instability of the first excited BM solution.
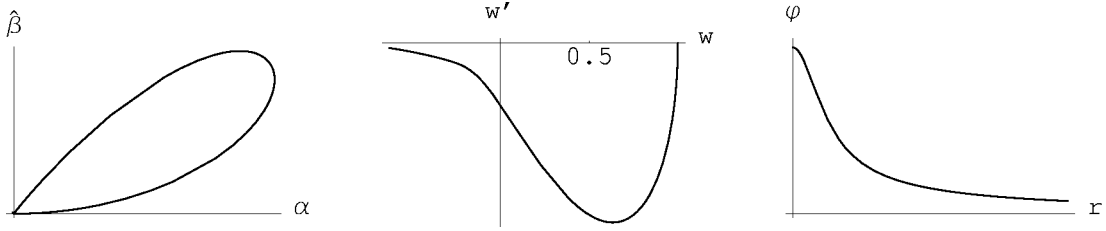
Figure 1: Reciprocal coupling limit: The ground state for $q = 8.49811$, $E = 0.377446$.
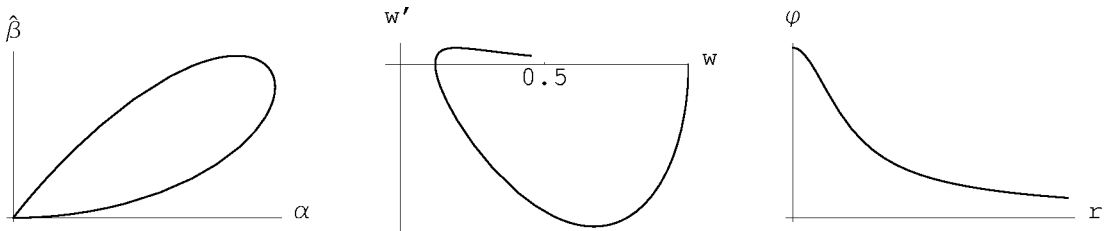
Figure 2: Reciprocal coupling limit: The first excited state for $q = 6.96132$, $E = 0.227762$.
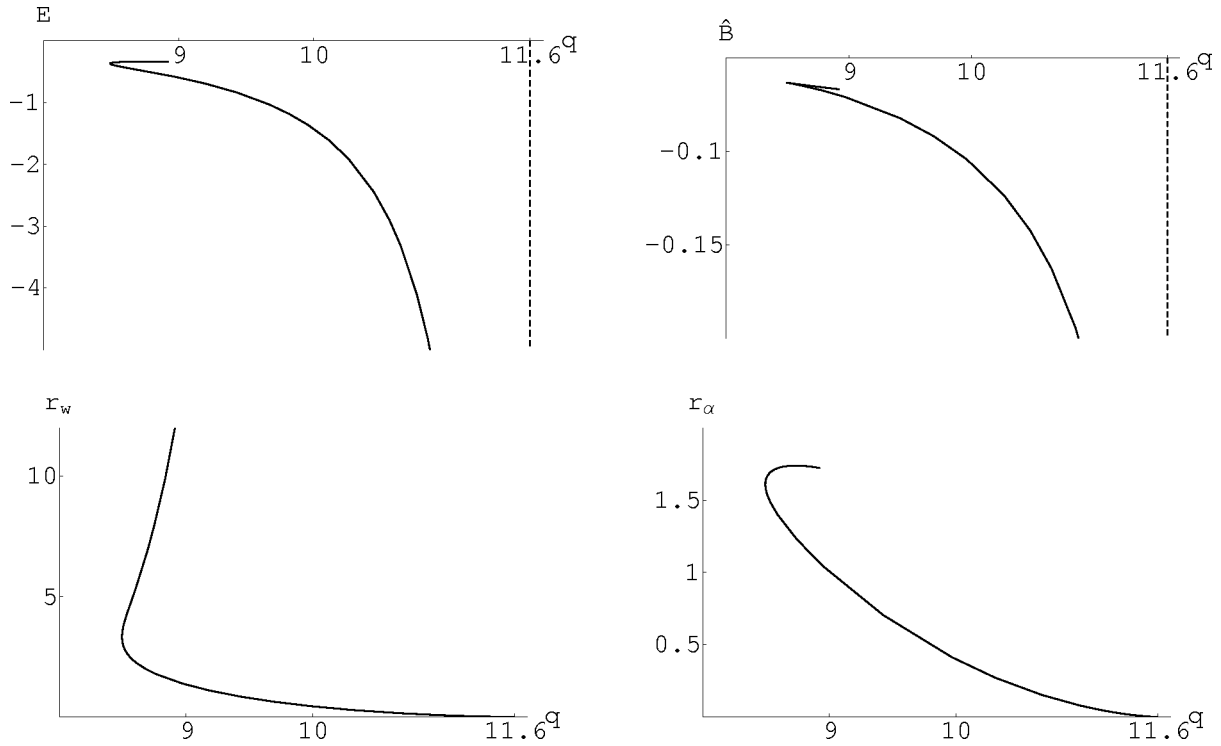
Figure 3: Reciprocal coupling limit: The energy spectrum and characteristic radii for the ground state
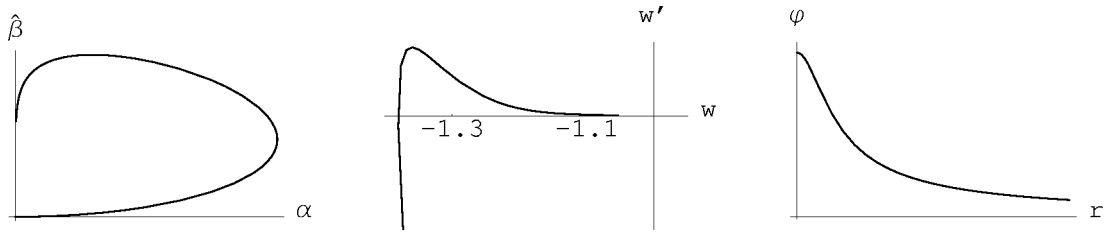
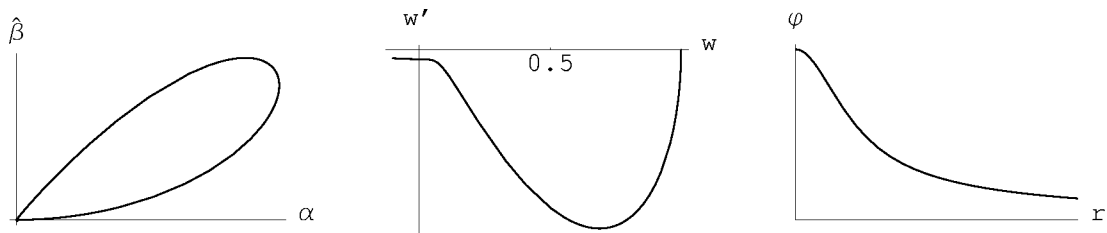Figure 4: Reciprocal coupling limit: The ground state for $q = 11.5838$, $E = 512161$.

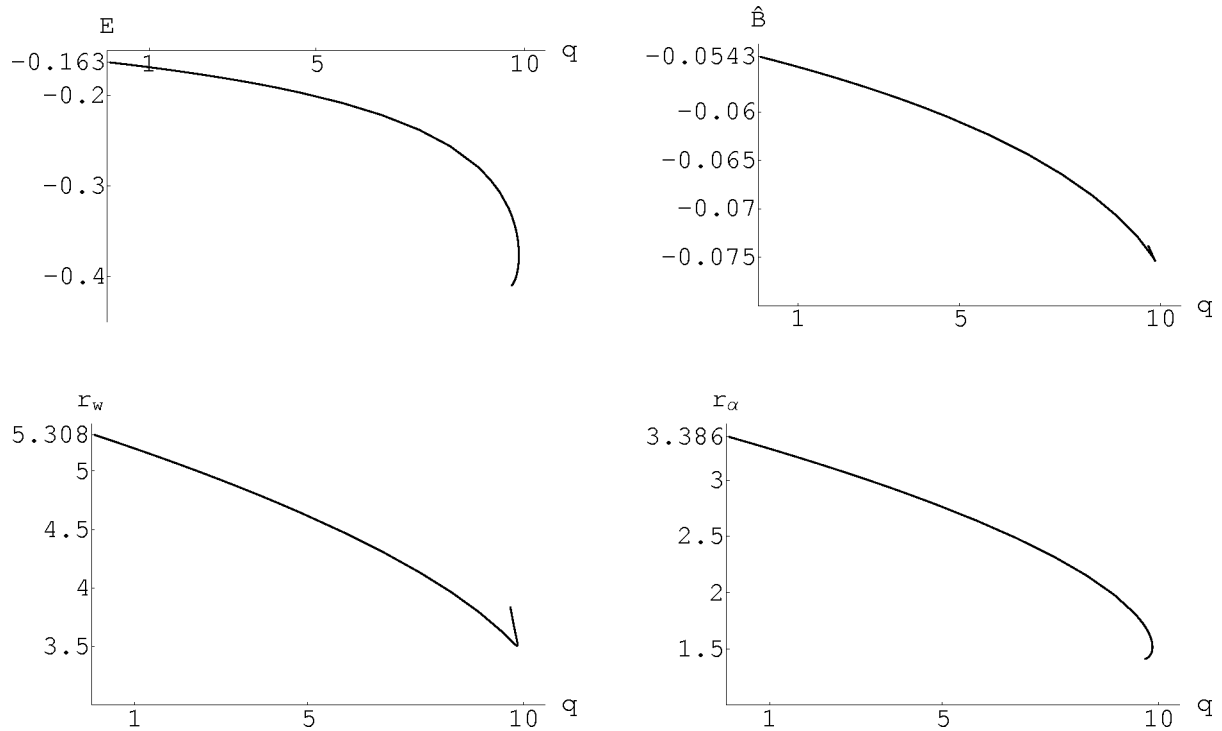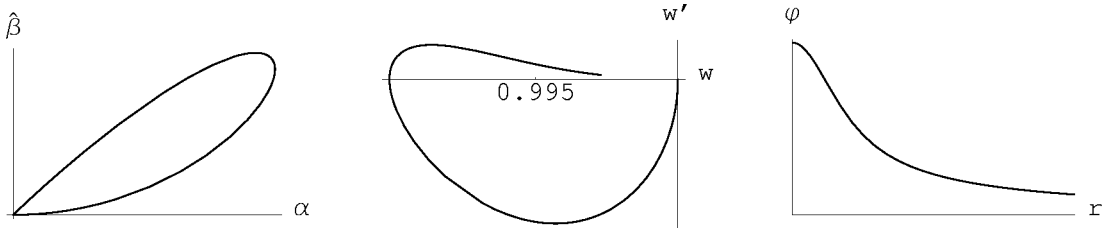Figure 5: Reciprocal coupling limit: The ground state for $q = 8.76701$, $E = 0.334974$.

Figure 6: Reciprocal coupling limit: The energy spectrum and characteristic radii for the first excited state

Figure 7: Reciprocal coupling limit: The first excited state for $q = 0.285092$, $E = 0.16431$.
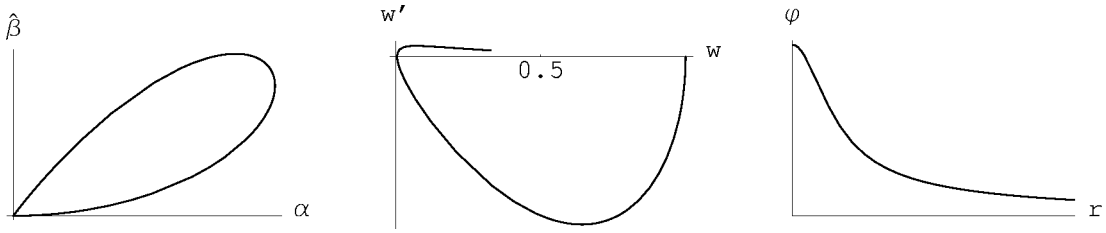
Figure 8: Reciprocal coupling limit: The first excited state for $q = 9.75946$, $E = 0.405186$.
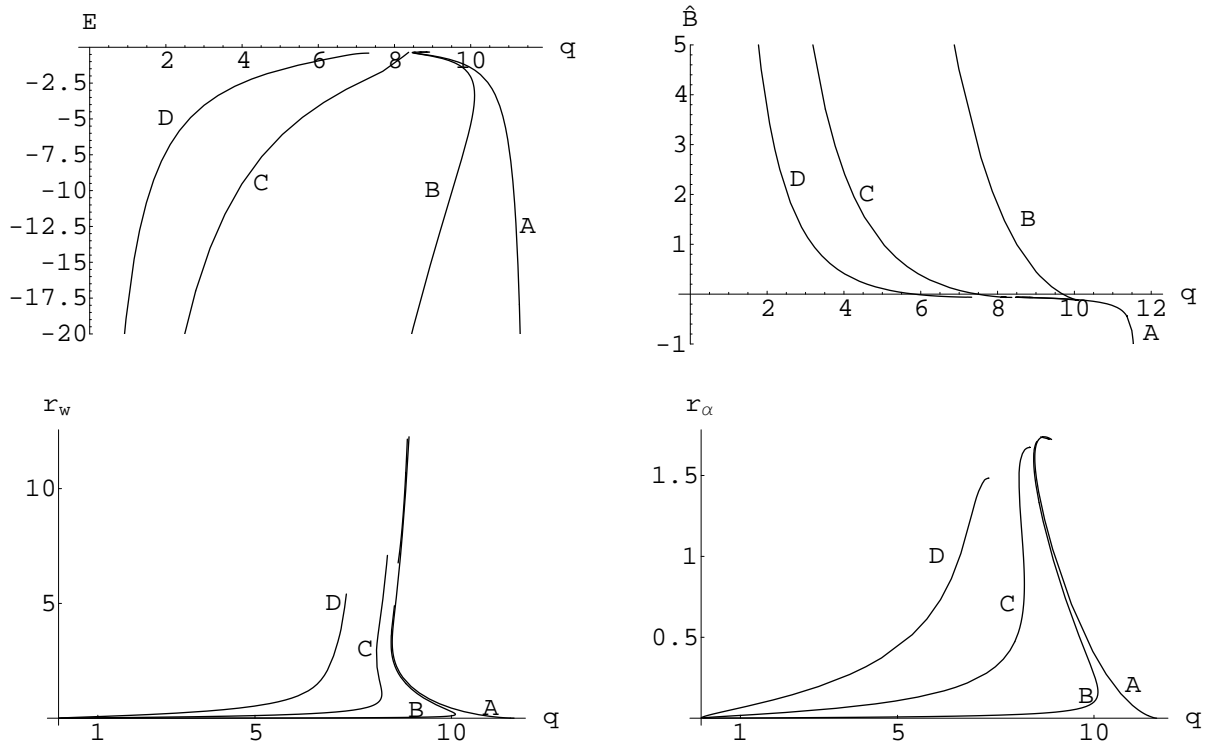
Figure 9: The energy spectrum and characteristic radii for the EDYM ground state and $\varepsilon = 0$ (A), $\varepsilon = 0.0003933$ (B), $\varepsilon = 0.005322$ (C), and $\varepsilon = 0.02067$ (D).
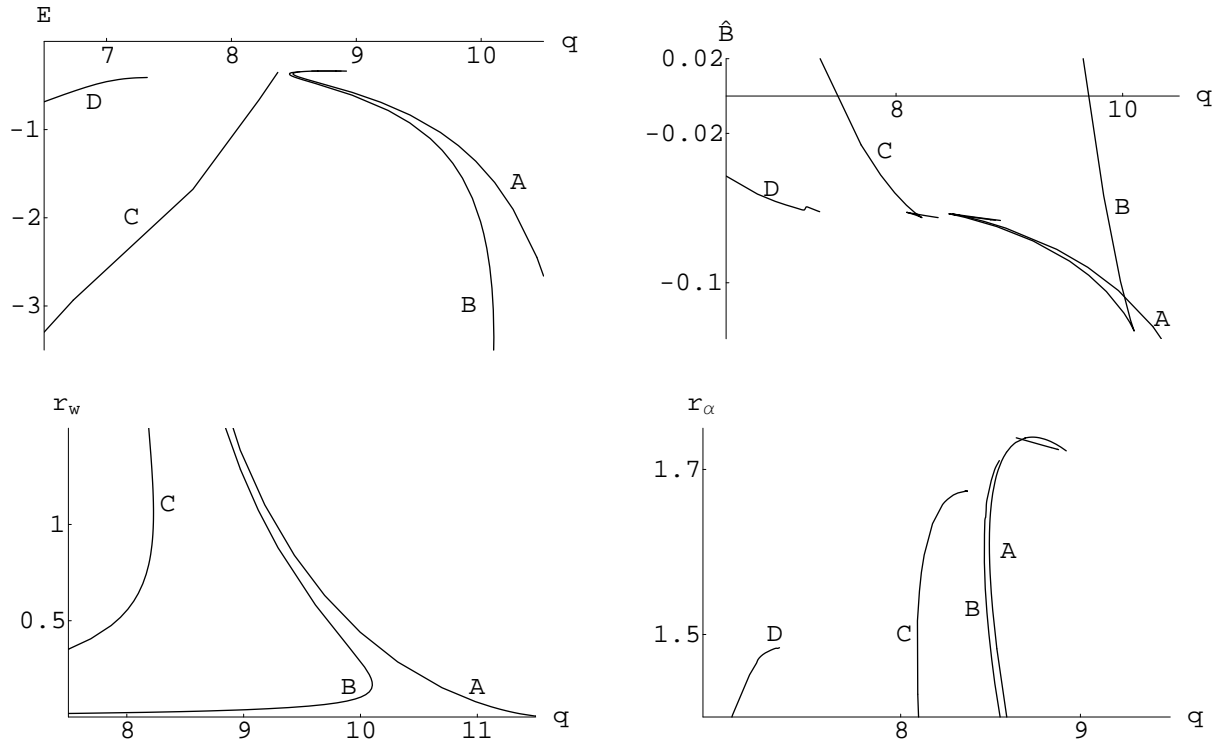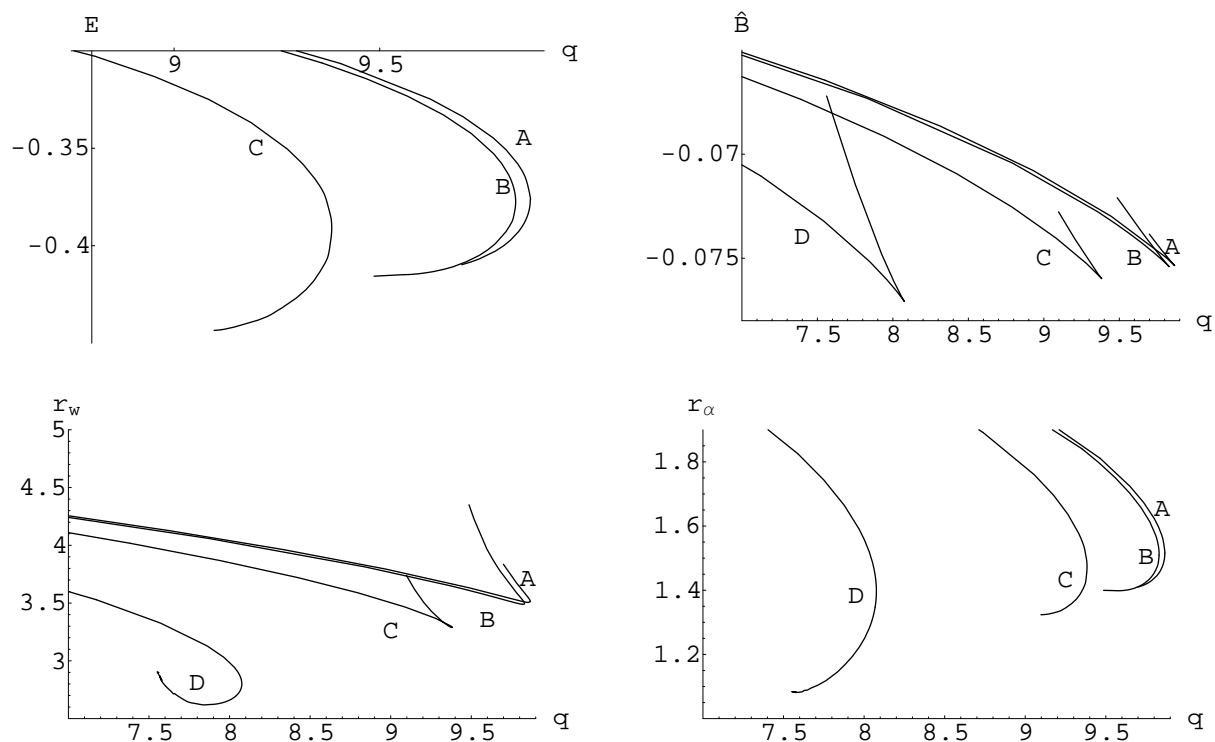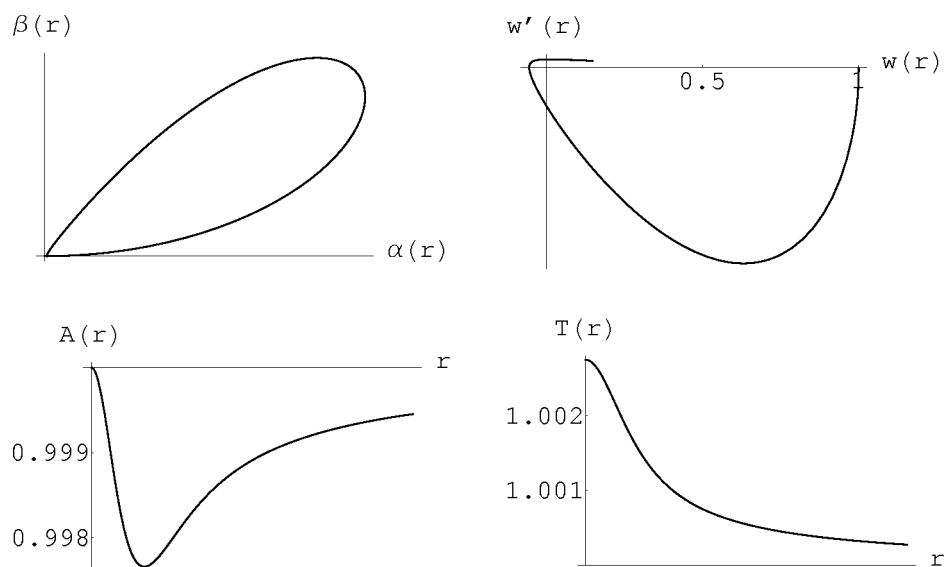
Figure 10: Details of the energy spectrum and characteristic radii for the EDYM ground state and $\varepsilon = 0$ (A), $\varepsilon = 0.0003933$ (B), $\varepsilon = 0.005322$ (C), and $\varepsilon = 0.02067$ (D).
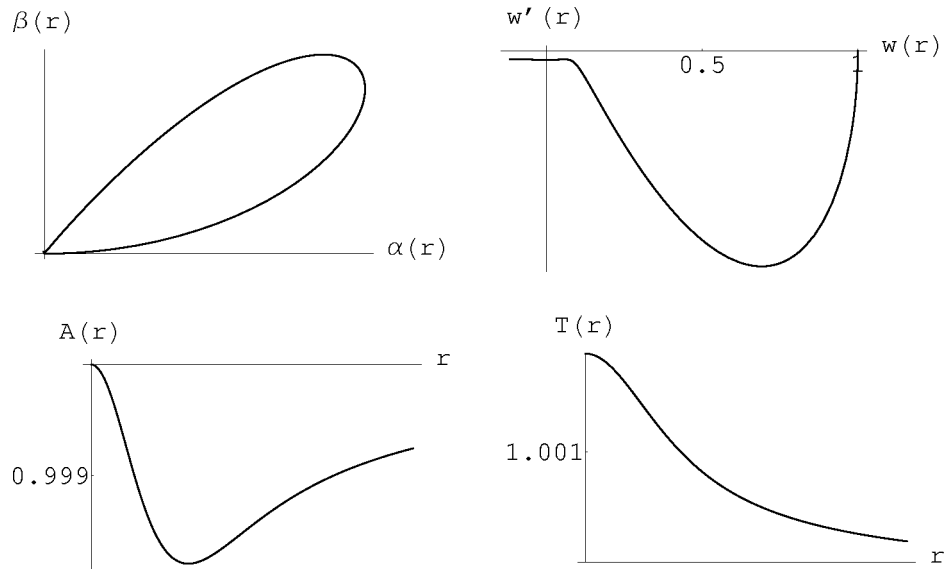
Figure 11: The EDYM ground state for $q = 8.8373$, $E = 0.3367$, and $\varepsilon = 0.0003933$.
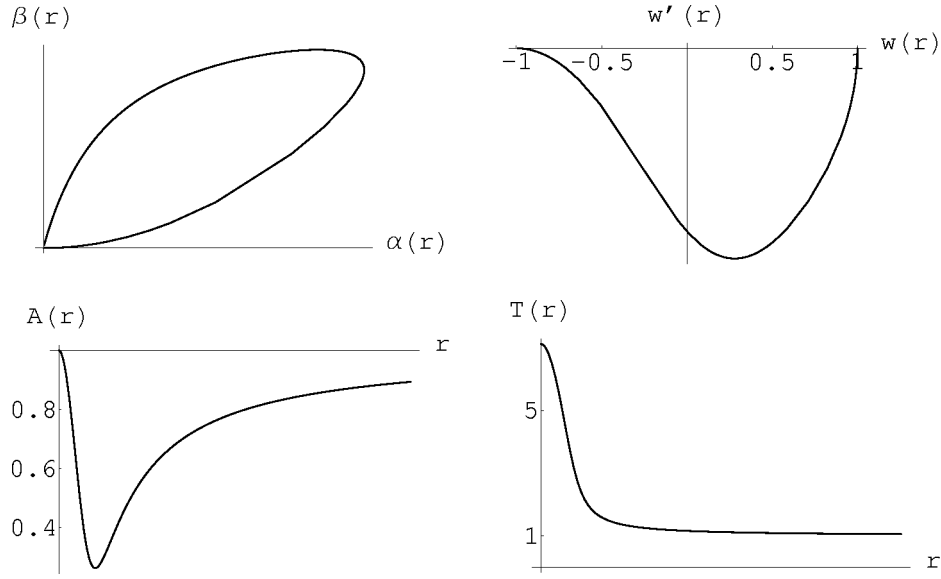
Figure 12: The EDYM ground state for $q = 0.005881$, $E = 17867.5$, and $\varepsilon = 0.005322$.
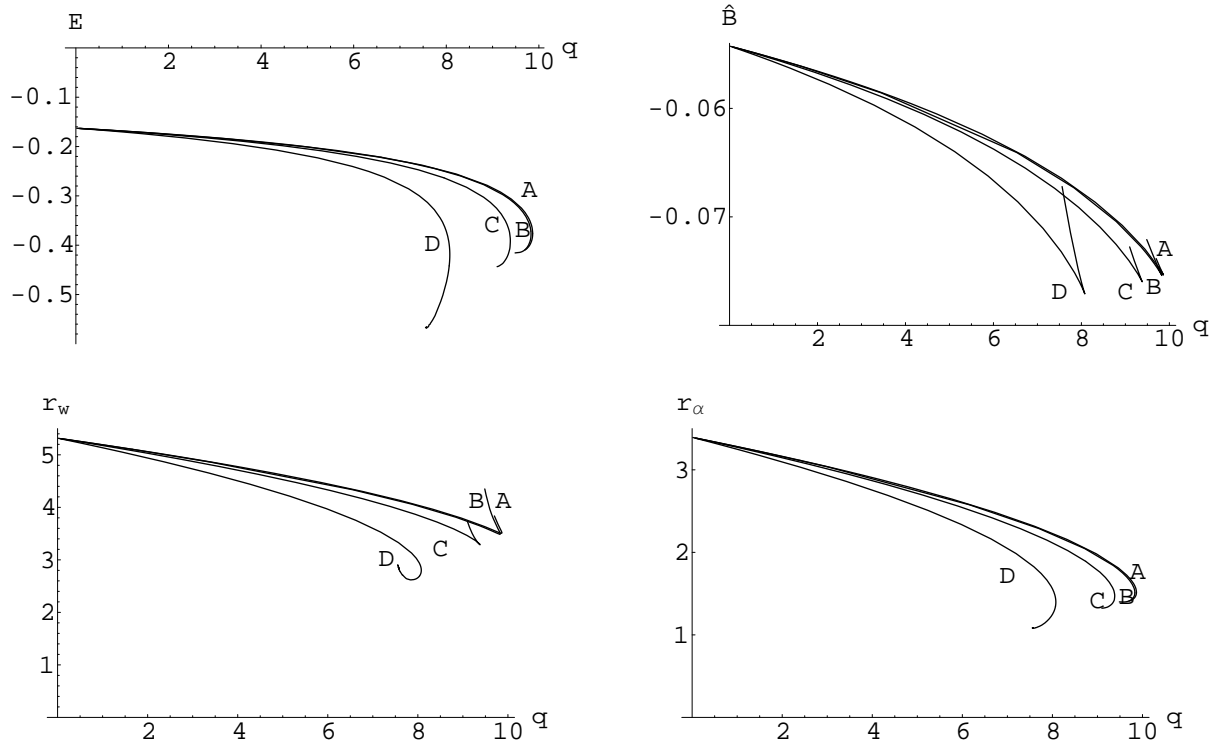
Figure 13: The energy spectrum and characteristic radii for the first excited EDYM state and $\varepsilon = 0$ (A), $\varepsilon = 0.0003933$ (B), $\varepsilon = 0.005322$ (C), and $\varepsilon = 0.02067$ (D).

Figure 14: Details of the energy spectrum and characteristic radii for the first excited EDYM state and $\varepsilon = 0$ (A), $\varepsilon = 0.0003933$ (B), $\varepsilon = 0.005322$ (C), and $\varepsilon = 0.02067$ (D).

Figure 15: The first excited EDYM state for $q = 9.548$, $E = 0.4153$, and $\varepsilon = 0.0003933$.
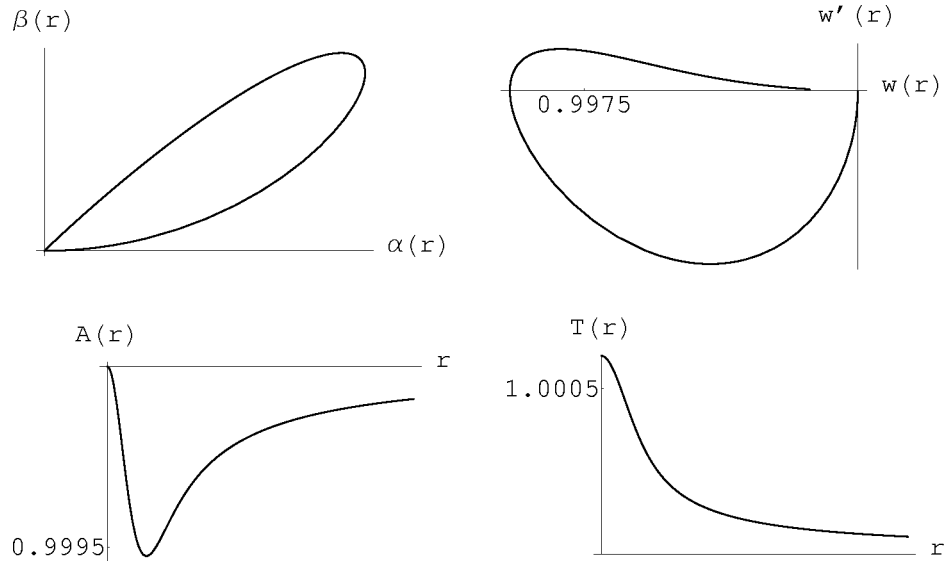
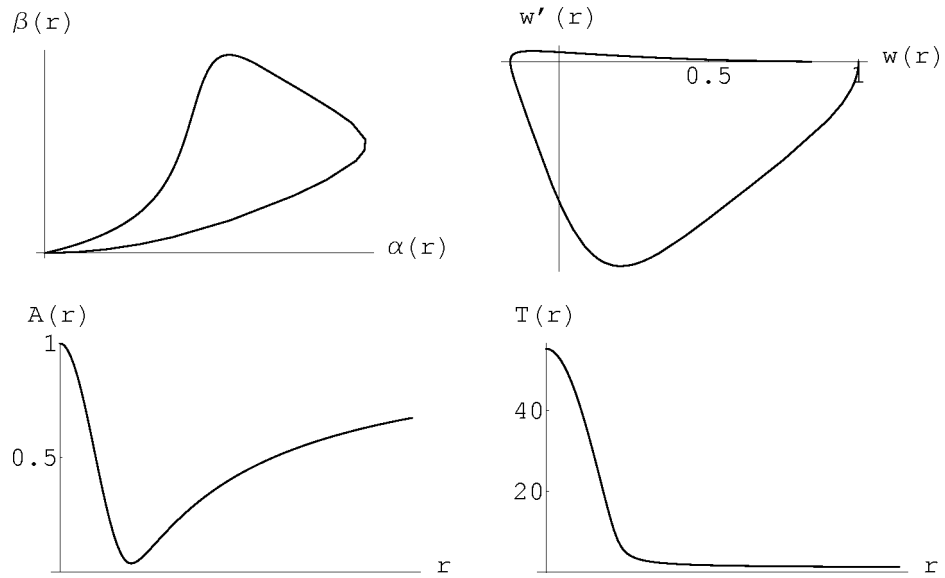Figure 16: The first excited EDYM state for $q = 0.09013$, $E = 0.1634$, and $\varepsilon = 0.02067$.

Figure 17: The deformation of the first excited BM state for $q = 0.00047737$, $E = 367616$, and $\varepsilon = 0.02067$.
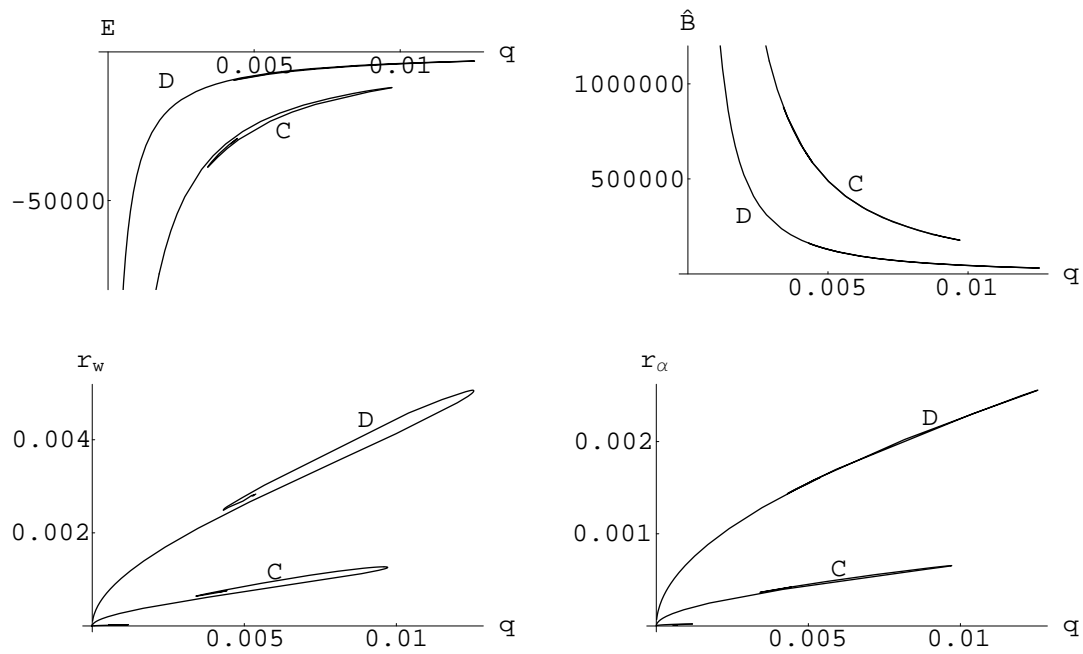
Figure 18: The energy spectrum and characteristic radii for the deformation of the first excited BM state for $\varepsilon = 0.005322$ (C) and $\varepsilon = 0.02067$ (D).
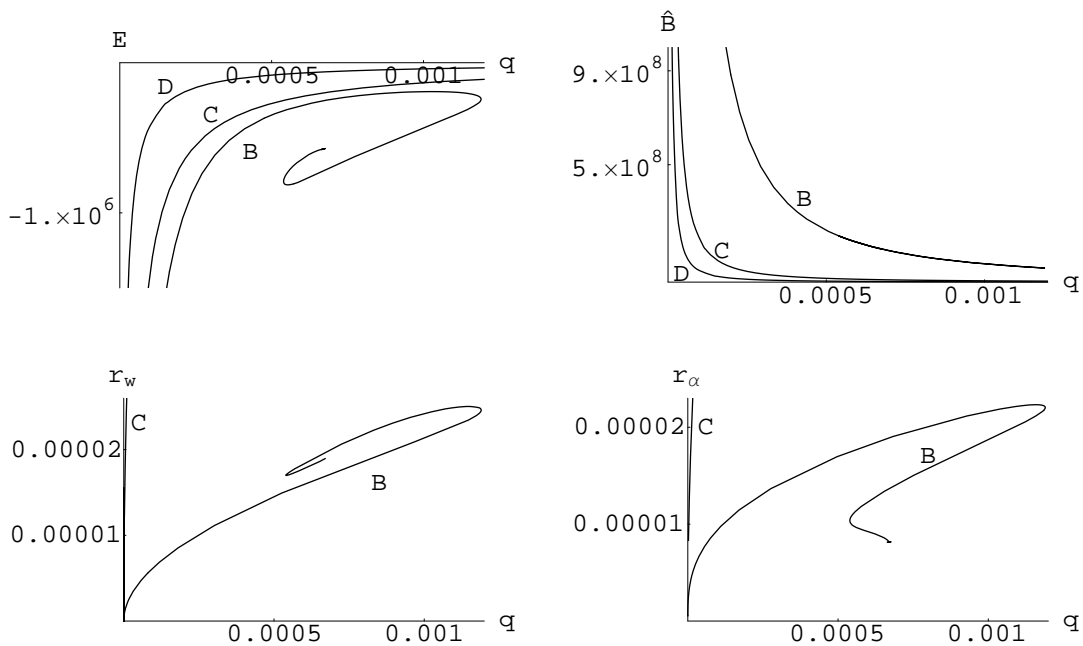

Figure 19: The energy spectrum and characteristic radii for the deformation of the first excited BM state for $\varepsilon = 0.0003933$ (B), $\varepsilon = 0.005322$ (C), and $\varepsilon = 0.02067$ (D).
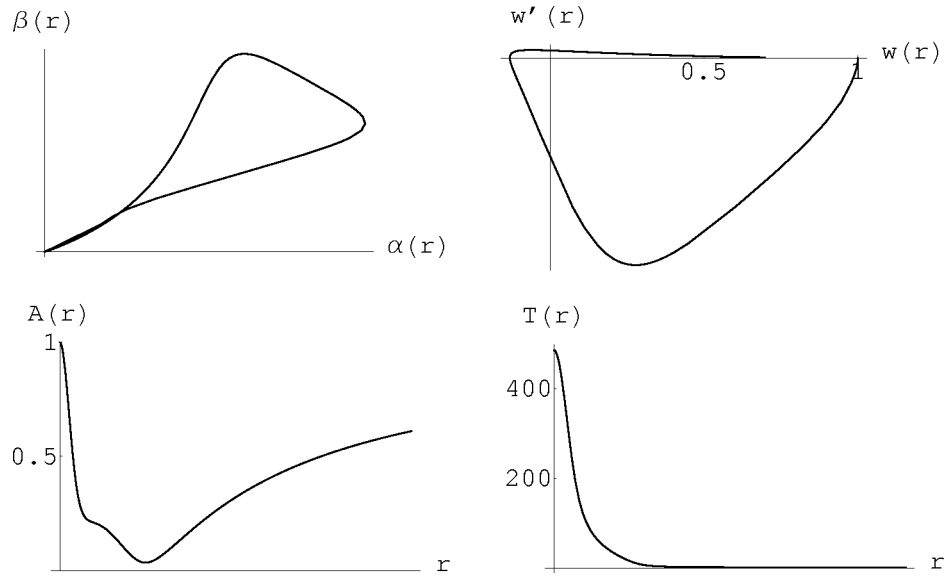
Figure 20: The deformation of the first excited BM state for $q = 0.0005528$, $E = 729921$, and $\varepsilon = 0.0003933$.
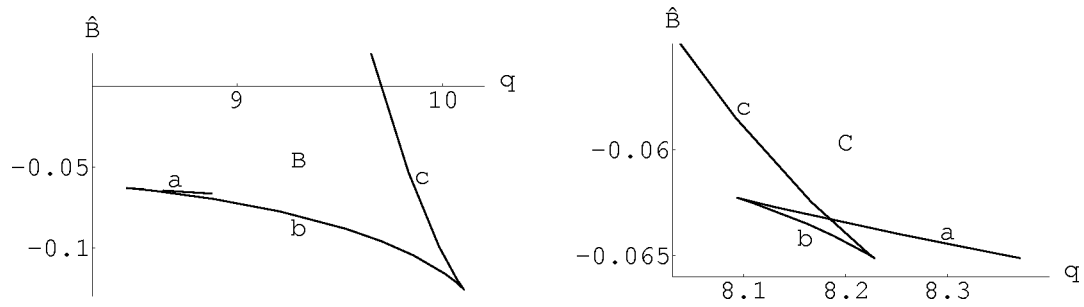

Figure 21: Detailed plots of the total binding energy of the EDYM ground state for $\varepsilon = 0.0003933$ (B) and $\varepsilon = 0.005322$ (C).

References

[1] Bartnik, R., and McKinnon, J., "Particlelike solutions of the Einstein-Yang-Mills equations," *Phys. Rev. Lett.* 61 (1988) 141-144

[2] Straumann, N,. and Zhou, Z., "Instability of the Bartnik-McKinnon solution," *Phys. Lett. B* 237 (1990) 353-356

[3] Finster, F., Smoller, J., and Yau, S.-T., "Particlelike solutions of the Einstein-Dirac equations," gr-qc/9801079, *Phys. Rev.* D 59 (1999) 104020

[4] Finster, F., Smoller, J., and Yau, S.-T., "Particlelike solutions of the Einstein-Dirac-Maxwell equations," gr-qc/9802012, *Phys. Lett.* A 259 (1999) 431-436

[5] Landau, L.D., Lifshitz, E.M., "Quantum Mechanics," Pergamon Press (1977)

[6] F. Finster, J. Smoller, and S.-T. Yau, "Non-Existence of Time-Periodic Solutions of the Dirac Equation in a Reissner-Nordström Black Hole Background," gr-qc/9805050, *J. Math. Phys.* 41 (2000) 2173-2194

[7] Yang, C.N., and Wu, T.T., "Some solutions of the classical isotopic gauge field equations," in "Properties of Matter Under Unusual Conditions," H. Mark and S. Fernbach eds., New York, Wiley Interscience (1969) 349-354

[8] Stoer, J., and Bulirsch, R., "Numerische Mathematik 2," 3rd edition, Springer (1990)

[9] Lee, T.D., "Mini-soliton stars," *Phys. Rev. D* 25 (1987) 3640-3657

[10] Smoller, J., "Shock Waves and Reaction-Diffusion Equations," 2nd ed., Springer (1994)

Felix Finster	Joel Smoller	Shing-Tung Yau
Max Planck Institute MIS	Mathematics Department	Mathematics Department
Inselstr. 22-26	The University of Michigan	Harvard University
04103 Leipzig, Germany	Ann Arbor, MI 48109, USA	Cambridge, MA 02138, USA
Felix.Finster@mis.mpg.de	smoller@umich.edu	yau@math.harvard.edu